

### **Author's response to referee #3:**

Thank you very much for the thorough, explicit, well organized, and practical comments. The review comes as an opportunity to improve the manuscript in various aspects. For convenience, the response is by order of appearance following the structure of the referee's report.

**Referee's comment #1a)** The motivation, strengths, and the central question of the paper could be made clearer in the introduction of the paper. As explained in Sect. 2, the region studied is interesting and different aspects are impacting the PBL height. The interesting aspects of the spatial variability of the studied region could be included in the introduction. In the light of the spatial variability, evaluating model performance on a single site would have limited value. One of the strengths of the study is the use of a network of ceilometers that can estimate the temporal development of the PBL at various locations simultaneously. This aspect deserves to be mentioned in the introduction.

**Author's response: Comment accepted.**

**Author's changes in manuscript:** The abstract and introduction paragraphed were changed accordingly.

**Referee's comment #1b)** The introduction does not provide enough information to motivate the development of a post-processing tool for the modeled PBL height. The goal to use ceilometer detected PBL height to correct for modeled PBL height could be simplified to "use A to correct B". Currently, it is demonstrated that to "use A" is possible, e.g. PBL height can, with some limitations, be retrieved from the ceilometer measurements. However, "to correct B" is neglected in the introduction. The introduction only states the need for accurate PBL estimate, but no literature on identified shortcomings, methods found for improvement or anything else that would have been done previously to evaluate or improve PBL height estimates in NWP models is presented. Do previous studies suggest that it is more feasible to correct the end product (e.g. the PBL height) than to improve model parametrizations in order to obtain a better result from the model? Do the authors envision a use for the corrected PBL height? The authors could also consider whether their main aim should be on developing a correction, or rather a rigorous evaluation of model performance in the complex region. The latter could be helpful for understanding model shortcomings and would be a more general result than a location and time specific correction.

**Author's response: Comment accepted.**

**Author's changes in manuscript:** The motivation of this study is to provide air pollution dispersion models with reliable input data of PBL heights. Weather models produce a high spatial and temporal resolution of PBL heights, albeit previous research has shown significant differences between the models' estimations and actual measurements. To overcome this obstacle, we established a correction tool for weather models by employing ceilometer measurements.

**Referee's comment #2)** One of the confusing aspects of this paper is the small number of days analyzed. The strength of the ceilometer is that data acquisition is cheap (see Sect. 1), however the small dataset is undermining this specific strength. The conclusions drawn are seriously undermined by the small sample size. For example, Sect. 6.2 seems to describe statistical results obtained from 13 data points. If possible, the authors should obtain more data. Alternatively, the study could be shifted to focus on case studies evaluating the shortcomings of the models in more detail. Although the reasons for focusing on daytime PBL only in summer are given, further selection seems to have taken place. Why are only 13 days included from August 2015, and 20 days from August 2016 (L. 292-293) in Sect. 6.1? Why does Sect. 6.2 only include 5 ceilometer sites, when Sect. 6.3 includes 8 ceilometer sites (L. 319-321 and 345-346)? Why do Sections 6.2 and 6.3 only include data from August 2015, and not from August 2016? Are the 13 days used in Sect. 6.2 a subset of the 33 days in Sect 6.1? The authors should provide an explanation for the small number of days analyzed and why certain days and sites were selected at different stages of the study.

**Author's response: Comment accepted.** The ceilometer array in Israel is a collection of ceilometers from different institutes. This study was the first attempt to gather data from all institutions. Unfortunately, some output files are missing. In other cases, the ceilometers operated for short periods. The database further narrowed down by removing days with dust storms or partial data. Eventually, we extracted the maximum days available for each ceilometer within six summer months: July-September 2015, and June-August 2016. We produced additional IFS and COSMO model runs to meet the periods available from the ceilometers. As a result, the analysis expanded from 13 specific days for 5 ceilometers to above 50 days for 6 ceilometers:

Ceilometer	# Days
Bet Dagan	91
Tel Aviv	122
Ramat David	123
Weizmann	55
Jerusalem	53
Nevatim	72

Hence, we combined sections 6.1 and 6.2 in section 5.1. Section 6.3 changed to Sect. 5.2.

[Author's changes in manuscript:](#)

The results and conclusions sections were changed considerably, as aforementioned.

[Referee's comment #3](#)) Related to the comment above about the amount of data, the authors should consider the statistical significance of the presented results. Specifically, wherever R-values are given (L. 298, Table 3, and elsewhere), the corresponding p-value should also be presented. Other techniques to analyze the statistical significance of the results are also welcomed, and the results should be discussed from the point of view of statistical significance.

[Author's response:](#) **Comment accepted.**

[Author's changes in manuscript:](#) Statistical analysis of boxplots, histograms, and tables added.

[Referee's comment #4](#)) Section 6.2 could provide possibly the most interesting results for considering model performance in terms of PBL height in complex environments. If model under- or overestimation could be connected to certain processes (e.g. the sea breeze), the results would be more generally interesting. Mountainous coastlines are not unique to Israel, and many people inhabit such areas. This section deserves a proper evaluation, and the analysis and discussion should be extended. Specifically, this section is hard to understand for someone not familiar with the geography of Israel. I would advise the authors to consider the presentation of their results. For example, the mean error at each site for each model and method could be presented with a symbol on a map having the color indicating the value. This would make any spatial structures in the mean, mean error (ME) or root mean square error (RMSE) more apparent. The authors could also plot the ME and/or RMSE as a function of the distance of the site to the shoreline and altitude above sea level (these are the two variables used for the correction in the next section). From the authors description of the situation, it seems that the

sea breeze has a clear influence on the PBL height. Is it to be understood, that the model does not correctly produce the sea breeze circulation, or is the model lacking in terms of the effect of the sea breeze on PBL height? It would be interesting if the authors could evaluate the discrepancy between ceilometer and model PBL height in terms of the strength, and spatial and temporal development of the sea breeze circulation during the day. Furthermore, in Sect. 6.3 data for 9-14 UTC are used, and I suggest the authors consider including the temporal development of the PBL height in their analysis in Sect. 6.2 as well.

**Author's response: Comment accepted.**

**Author's changes in manuscript:** As described in response to comment #3, this section was changed dramatically following the referee's suggestions.

**Referee's comment #5a)** Before a correction is developed and presented, it should be made clear that a correction is needed and that there is a systematic bias that can be corrected for. Table 3 (and Section 6.1) show that the mean error of COSMOR compared to radiosondes is -3 m, which does not leave much room for improvement. Also Table 5 shows that at different sites the mean error of COSMOR is within a few tens of meters at most. (However, I would be cautious to draw conclusions from statistics comprising of 13 data points, and the authors should obtain a larger sample size if possible. See comments 2 and 3). For a 1 km deep PBL, an error of 30 m is 3%. For which application is this not good enough, and how good should the model performance be? Furthermore, considering that the definition of the planetary boundary layer is slightly ambiguous, can a perfect agreement between different methods be expected? The authors should explain why they think the model performance is not good enough and requires improvement. Furthermore, the authors could consider if the correction they presented would actually be more useful for the IFS model that shows clearly worse performance than the COSMO in terms of PBL height prediction.

**Author's response: Comment accepted.**

**Author's changes in manuscript:** With great effort, we obtained a larger sample size. Now, the necessity to improve the models' PBL heights is evident from the statistical analysis. The primary purpose of this study was to improve the performance of air pollution dispersion models by providing reliable PBL heights from NWP models. In some cases (Uzan et al., 2012), a height difference of 100 m between the actual PBL height and the models' assessments affect ground-level air pollution concentrations significantly. Therefore, the correction tool is useful for both regional and global models.

Uzan, L. and Alpert, P.: The coastal boundary layer and air pollution - a high temporal resolution analysis in the East Mediterranean Coast, *The Open Atmospheric Science Journal*, 6, 9–18, 2012.

**Referee's comment #5b)** Sect. 6.2 should demonstrate the basis of the correction presented in Sect. 6.3. The fact that the mean error in Tel Aviv, Beit Dagan and Weizmann are so similar suggests a spatial consistency that is more clear for COSMOR than COSMOP. (Table 5). Is this the reason COSMOR was used for the correction in Sect. 6.3 instead of COSMOP? The fact that there seems to be some spatial structure in the mean error is promising for developing a correction. The RMSE does not seem so spatially consistent.

**Author's response: Comment accepted.**

**Author's changes in manuscript:** The new results section reveals which model and method produced the best results following the ceilometers' locations.

**Referee's comment #5c)** To justify the correction method presented in Sect. 6.3, it should be established that a bias exist in the models' PBL height estimation that depends on altitude and distance from shoreline, that could consequently, be corrected for. The authors should evaluate how the discrepancy between ceilometer and model PBL height depends on the topography and distance from shoreline. Furthermore, this could be done for different hours of the day, as the correction procedure is also applied for each hour separately.

**Author's response: Comment accepted.**

**Author's changes in manuscript:** Section 6.3 changed to 6.2, including an elaborate explanation of the correction tool performance for a single day study case between 9-14 UTC. Figures for each hour display the models' estimations, PBL heights after correction, and cross-validation examination for Bet Dagan and Jerusalem.

**Referee's comment #6)** Perhaps the most serious shortcoming of the manuscript is that it is not demonstrated that the model result is better after correction. The authors should include a quantitative evaluation of the improvement of the model PBL after the correction. For example, the radiosondes at Beit Dagan could be used as an independent reference for the model PBL height. Another approach would be to estimate the correction parameters using only some of the available ceilometer stations, and using the remaining stations as a references to estimate the improvement in PBL height achieved by the correction. Varying the number of stations and

the locations of the stations included for fitting the correction parameters also give an indicator for how many ceilometers needs to be included, or how they need to be located, for achieving a significant improvement for the COSMOR PBL height. If the authors aim is to show that the ceilometer is a useful tool to improve the modeled PBL height, the strength of their paper relies on the extent and rigor that this kind of analysis is carried out.

**Author's response: Comment accepted.**

**Author's changes in manuscript:** Cross-validation analysis demonstrated the efficiency of the correction tool. The improvements were discussed in the conclusions according to the new results section (see responses to comments #2 and #5c).

**Referee's comment #7a)** More attention should be paid to make the reasoning understandable for readers that are not so familiar with the specific geography and climatology of the region. Firstly, the studied region and its interesting aspects could be mentioned in the introduction. The first time the location is given is the very end of the introduction, on line 97. This should be included already in the previous paragraph that outlines the purpose of the study, as well as in the abstract.

**Author's response: Comment accepted.**

**Author's changes in manuscript:** The spatial variability and locations were added to the abstract and introduction.

**Referee's comment #7b)** A topography map should be included. Global topography data is available (for example from NOAA <https://doi.org/10.7289/V5C8276M>) and a map can be drawn using openly available tools (such as python).

**Author's response: Comment accepted.**

**Author's changes in manuscript:** A topographical map was added.

**Referee's comment #7c)** Depending on the weight the authors want to give to the humidity (mentioned on lines 103-104) and the prevailing synoptic conditions (line 125), they could also include a map of mean precipitation and pressure in August to help the reader to follow their argumentation.

**Author's response:** The manuscript modifications doubled the number of figures. Therefore, we preferred to add references instead of maps.

**Author's changes in manuscript:** Additional references of previous research in Israel describing the dry summer season.

**Referee's comment #8)** L.1-2: The authors should reconsider the title of the manuscript. The current title is somewhat misleading because it implies that the correction for PBL height was considered for both models, when in the manuscript only the COSMO PBL height was corrected. Furthermore, the journal guidelines recommend avoiding the use of abbreviations in the title, so the authors might want to avoid the use of "NWP" in the title.

**Author's response: Comment accepted.** The research studies two NWP models and established a correction formula feasible for both models. Thus, we find it appropriate to mention IFS in the title as well.

**Author's changes in manuscript:** "NWP" was removed from the title.

**Referee's comment #9)** L.23-25: Here results are given for flat and elevated terrain. Consulting Tables 4 and 5 it seems that flat terrain refers to Tel Aviv, and elevated terrain to Jerusalem. The authors should consider mentioning the sites for which the numbers refer to avoid ambiguity, or at least mention that the values presented are from single stations.

**Author's response: Comment accepted.**

**Author's changes in manuscript:** The titles in the new results section refer to each ceilometer.

**Referee's comment #10)** The abstract does not mention Israel or give any other indication over the geographic locations apart from "heterogeneous area" and mention of the Beit Dagan radiosonde launch site. Location should be given.

**Author's response: Comment accepted.**

**Author's changes in manuscript:** Locations were added to the abstract.

**Referee's comment #11)** L.33-40: Considering that this paragraph states the broad motivation and importance of this study, some references would be appropriate.

**Author's response: Comment accepted.**

**Author's changes in manuscript:** References were added.

**Referee's comment #12)** L.56-57: "ceilometers obtain a wide spatial resolution per lidar" - I'm afraid I do not understand the meaning of this phrase. Perhaps the authors mean that a wider spatial resolution is achieved by ceilometers than lidars?

**Author's response: Comment accepted.**

**Author's changes in manuscript:** The text was changed accordingly.

[Referee's comment #13](#)) L.53-65: This paragraph seems to suggest that ceilometers are better than lidars in every aspect. It would be fair to mention a shortcoming of the ceilometer compared to a lidar.

[Author's response](#): **Comment accepted.**

[Author's changes in manuscript](#): The shortcomings of ceilometers were added to the introduction section.

[Referee's comment #14](#)) L.89-91: It is not obvious here why the summer season is more appropriate for an approach that is limited by precipitation. It is later explained that this season has low precipitation. This should also be mentioned here to help the readers not familiar with local climatology.

[Author's response](#): **Comment accepted.**

[Author's changes in manuscript](#): The meteorological conditions were added to the introduction section.

[Referee's comment #15](#)) L.92-97: It would be possible to help the reader further by outlining the structure of Sect. 6, either here or at the beginning of Sect. 6.

[Author's response](#): **Comment accepted.**

[Author's changes in manuscript](#): The outline was elaborated accordingly.

[Referee's comment #16](#)) L.85-86: The introduction demonstrates the strengths of ceilometers compared to other available observational techniques to estimate PBL height, but only states that ceilometers have not been used often for evaluating model performance. However, other observational techniques have, and this should be mentioned. Specifically, have other observational tools been used for evaluating PBL height in NWP models in Israel, or other mountainous coastlines?

[Author's response](#): **Comment accepted.**

[Author's changes in manuscript](#): Information regarding the observational tools implemented for COSMO PBL height evaluation was added in the introduction section.

[Referee's comment #17](#)) I find the extent of presenting the literature for the use of ceilometer to detect PBL height satisfactory. However, no mention of previous work using ceilometer to



derive PBL height in Israel is presented. The authors should cite at least Uzan et al. (2016) and any other studies employing the measurement technique in their region of study.

**Author's response: Comment accepted.** As discerned by the referee, we were first to employ ceilometers for PBL height detection in Israel (Uzan et al., 2016). Up until our research, the ceilometers' in Israel were acknowledged merely as ceiling height detectors. Thus, historical data had neither been acquired or saved. The data we received was collected following our specific request. It was the maximum amount of data available. This explains the inevitable situation of low data availability for spatial analysis limited to the summer season.

**Author's changes in manuscript:** Uzan et al. (2016) was cited in the introduction.

**Referee's comment #18)** L.106: "IMS weather reports" - The authors should provide a more specific reference, if possible.

**Author's response: Comment accepted.**

**Author's changes in manuscript:** "Israeli Meteorological Service relative humidity climate report 1995-2009, <https://ims.gov.il/en/ClimateReports>".

**Referee's comment #19)** L.100-103: Here could cite Fig. 1.

**Author's response: Comment accepted.**

**Author's changes in manuscript:** Fig 1 was cited accordingly.

**Referee's comment #20)** L.111: PBL height detection becomes increasingly difficult with increasing range (because of the decrease in the signal-to-noise ratio), and because of the low power of the ceilometer deep boundary layers are hard to detect. The moderate PBL height means that it is less of an issue in this study, and the authors could mention this to support their choice of instrumentation.

**Author's response: Comment accepted.**

**Author's changes in manuscript:** The comment was added to the text. Thank you.

**Referee's comment #21)** L.112-115: "Summer dust outbreaks in the eastern Mediterranean are quite rare (Alpert and Ziv 1989, Alpert et al., 2000) therefore, they were not addressed here, especially in the height levels below 1 km (Alpert et al., 2002)." - The sentence structure is unclear. Do the authors mean that especially dust outbreaks below 1 km were not addressed,

or perhaps that the dust outbreaks below 1 km were especially rare and therefore not addressed?  
Should be clarified.

**Author's response: Comment accepted.**

**Author's changes in manuscript:** The sentence was clarified in the text.

**Referee's comment #22)** L.119: The abbreviation LST is not defined.

**Author's response: Comment accepted.**

**Author's changes in manuscript:** LST = UTC+2 was added to the text.

**Referee's comment #23)** L.116-138: This is a paragraph about PBL structure and development in the studied region based on literature. It is useful and informative, even though it is concise and provides a lot of information for someone not familiar with the region. This paragraph is crucial for understanding the results, and the authors should not be afraid to extend if necessary to better understand the results. They should also refer back to this section at later parts of the manuscript when the concepts described are discussed. Furthermore, Fig. 3b could also be referred to as an example to aid the description of the diurnal cycle.

**Author's response: Comment accepted.**

**Author's changes in manuscript:** Changes were made according to the figures and text of the new results section.

**Referee's comment #24)** L.116-138: The use of abbreviations seems excessive: SBF and RL are only used once after being introduced, and could therefore omitted. Also CBL and SBL are only used 1-2 times after this paragraph and the need for the abbreviations is questionable and does not aid readability of the manuscript.

**Author's response: Comment accepted.**

**Author's changes in manuscript:** The abbreviations-SBF, SBL, CBL, and RL were removed.

**Referee's comment #25)** L.136-138: Please provide reference(s) for nocturnal PBL in Israel, if available.

**Author's response:** Previous studies of the nocturnal PBL in Israel were conducted in regions not in the scope of our research, therefore, they were not cited.

**Author's changes in manuscript:** No change was made.

[Referee's comment #26](#)) Sect. 4.1: The placement of ceilometers in the heterogeneous research area should be described. Do the ceilometer sites adequately represent the variability of the region? Are the different regions mentioned in the text (humid, arid, coastal, complex terrain) covered by the measurements?

[Author's response](#): **Comment accepted.**

[Author's changes in manuscript](#): The region of the ceilometers was added in the relevant sections.

[Referee's comment #27](#)) Sect.5.3: The ceilometer backscatter profile is related to the aerosol loading, and therefore the layer that is detected is actually an aerosol layer. Implicit in the method described is the assumption that the PBL height corresponds to the height of the aerosol layer directly above ground. This assumption should be stated, and potential consequences to the results discussed. It is especially a limitation for detecting internal boundary layers which might develop due to the sea breeze circulation or katabatic winds.

[Author's response](#): **Comment accepted.**

[Author's changes in manuscript](#): An explanation was added to Sect. 1.

[Referee's comment #28](#)) L.143: Table 2 is mentioned before Table 1 in text, the order of the tables should be swapped.

[Author's response](#): The explanation of the research area was moved to the introduction section therefore, it wasn't necessary to swap the table numbers.

[Author's changes in manuscript](#): No change made.

[Referee's comment #29](#)) L.156: The authors could consider using the word "increased" rather than "improved" because it is more neutral. Although the model performance might have improved in important aspects due to increase in resolution, the computational cost likely did not.

[Author's response](#): **Comment accepted.**

[Author's changes in manuscript](#): The section was rephrased.

[Referee's comment #30](#)) L.163-164: "The spatial resolution of the models affects their ability to refer to the actual topography rather than a smoothed grid point." Is this the reason that the ceilometer site is used as a parameter for correction? If so, it should be clarified.

**Author's response: Comment accepted.**

**Author's changes in manuscript:** An explanation was added to the new summary and conclusions section.

**Referee's comment #31)** L.164-165: "the models' results were corrected by the actual ground base heights for each measurement site" - Unfortunately, I cannot follow here. Presumably the correction meant here is not the correction presented in Sect. 6.3. Perhaps the authors mean that the model levels were adjusted based on the precise altitude of each ceilometer station? Clarification would be appreciated.

**Author's response: Comment accepted.**

**Author's changes in manuscript:** Additional text: "Therefore, the models' levels were adjusted based on the precise altitude of each ceilometer station."

**Referee's comment #32)** L.144-162: Considering that IFS provides boundary conditions for COSMO, and that the description of the COSMO model refers to IFS model parameterizations, the authors could consider switching the order of introducing the two models. e.g. move lines 156-165 before line 144.

**Author's response: Comment accepted.**

**Author's changes in manuscript:** The order was changed. IFS was introduced before COSMO.

**Referee's comment #33)** L.157: It seems that the IFS has more vertical levels, but does it have better vertical resolution in the boundary layer? Information on vertical resolution should be added in Table 2.

**Author's response: Comment accepted.**

**Author's changes in manuscript:** The information was added to Table 2.

**Referee's comment #34)** L.188-189: "In order to derive the backscatter coefficient from ceilometer measurements, signal calibrations and water vapor corrections are necessary" - It is not clear if the corrections were done (presumably not), and should be clarified.

**Author's response: Comment accepted.**

**Author's changes in manuscript:** The sentence was rephrased.

[Referee's comment #35](#)) L.193-194: It could be mentioned that averaging multiple profiles improves the signal-to-noise ratio and thereby is likely to also improve the detection of the PBL height.

[Author's response](#): **Comment accepted.**

[Author's changes in manuscript](#): The sentence was rephrased.

[Referee's comment #36](#)) L.197: The overlap effect is a well-known issue for lidar systems, however, the authors could provide a reference.

[Author's response](#): **Comment accepted.**

[Author's changes in manuscript](#): A reference was added: "At these heights, a constant perturbation existed due to the overlap of the emitted laser beam and the receiver's field of view (Weigner et al., 2014)".

[Referee's comment #37](#)) L.215-217: "the radiosonde's horizontal position is under  $0.01^\circ$  which is an order of magnitude from the models' grid resolution" - This is true for IFS but not for COSMO, which has a resolution of  $0.025^\circ$ . The authors should be more specific to avoid a misleading statement.

[Author's response](#): **Comment accepted.**

[Author's changes in manuscript](#): The text was rephrased.

[Referee's comment #38](#)) L.239-241: The method used for COSMO, why two different thresholds are needed, and how it differentiates from that used in for IFS or the radiosondes is not clear. What is the reason for applying a different criterion for COSMO than the IFS and soundings?

[Author's response](#): **Comment accepted.** IFS adapted a single threshold of 0.25 following the conclusions of (Seidal et al.,2015). The COSMO model refers to 0.33 for stable atmospheric conditions (Wetzel, 1982), and 0.22 for unstable conditions by 0.22 (Vogelezang and Holtslag, 1996).

[Author's changes in manuscript](#): The information was added to the text.

[Referee's comment #39](#)) L.282-283: "This height indicates the entrainment zone rather than the actual cloud top." For anything than the most optically thin clouds, the ceilometer signal attenuates before reaching the cloud top. Therefore, the ceilometer is very unlikely to be detecting cloud top.

**Author's response:** **Comment accepted.** We must clarify we didn't attempt to claim the ceilometer detects the cloud top. On the contrary.

**Author's changes in manuscript:** The sentence was rephrased to avoid the misunderstanding.

**Referee's comment #40)** L.292-293: Considering the change in IFS resolution between 2015 and 2016, is it appropriate to evaluate the IFS data together, or should data from 2015 be considered separately from 2016?

**Author's response:** In 2015 and 2016 the ceilometers were indicated by the same grid points and horizontal levels. Therefore, we did not find it necessary to separate the results. Furthermore, we ran the analysis separately for 2015 and 2016. The difference between the results was insignificant.

**Author's changes in manuscript:** No changes made.

**Referee's comment #41)** L.310-314: In the introduction it is mentioned that Ketterer et al. (2014) found poor correlation between ceilometer PBL height and the PBL height from COSMO. Why is their result so different from that found here?

**Author's response:** **Comment accepted.** The main difference is the research area. Ketterer et al., (2014) studied complex topography of the Swiss Alps (two sites, 3,580 m a.s.l and 2,061 m a.s.l), whilst our study region was confined between the shoreline to highest point of 830 m a.s.l.

**Author's changes in manuscript:** To avoid a too-long introduction section, we moved the discussion of previous research (Ketterer et al., 2014 and Collaud et al., 2014) to the results section.

**Referee's comment #42)** As far as I can see in Fig. 2, the gap between IFSP and RS is even larger for the data point indicated by the red rectangle in the figure below. I appreciate that the authors give an explanation to the anomalous PBL height on the 17 Aug 2016, but I'm concerned that this paragraph is slightly misleading. I'm not convinced that the difference between the IFSP and RS is the largest on 17 Aug 2016. I suggest the authors re-formulate this paragraph with the emphasis on giving an explanation for the anomalous PBL on 17 Aug 2016, rather than claiming this is the day with largest discrepancies, or alternatively provide an objective measure for a "largest gap" and an explanation why the large discrepancy in IFSR is worth considering but the even larger discrepancy in IFSP on another day is omitted. Based on

the next section, I could guess that these data points indicated by the red box are from 10 Aug 2015 (Fig 4b). If so, please include this information in this section of the manuscript.

**Author's response: Comment accepted.** The new results section consists of new figures according to the referee's comments 2-6.

**Author's changes in manuscript:** The data of Fig. 2 and new for other ceilometers was analyzed to produce new compelling figures.

**Referee's comment #43)** Sect 6.1. No discussion about the differences between bulk Richardson and parcel method is included. From Tables 4 and 5 it seems like IFS results are more sensitive to the choice of method. Perhaps the authors could discuss these results.

**Author's response: Comment accepted.**

**Author's changes in manuscript:** The new results section consists of a discussion on the different methods.

**Referee's comment #44)** Sect 6.1: As far as I can understand, the main purpose of this chapter is to demonstrate the feasibility of ceilometer measurements to use for model evaluation. The authors could consider using this 33 point data set to compare the model results to the ceilometer to see if the results are similar than those obtained in comparison with the radiosondes to give additional confidence.

**Author's response: Comment accepted.**

**Author's changes in manuscript:** The results section was changed accordingly.

**Referee's comment #45)** L.324-330: If the 13 days evaluated in Sect 6.2. are also included in the analysis of Sect 6.1, this paragraph does not provide any new information. For the clarity of the manuscript, I would advise the authors to include all comparison of radiosonde with other data in Sect 6.1, and focus on the spatial analysis in Sect. 6.2, as indicated by the title.

**Author's response: Comment accepted.**

**Author's changes in manuscript:** The results section was changed accordingly.

**Referee's comment #46)** L.331: "By and large, COSMOR achieved the best statistical results" - This statement seems overemphasized. In terms of root mean square error, COSMOP performed better on 4 of the 5 sites presented, and the mean error was better for 2 sites.

**Author's response: Comment accepted.**

**Author's changes in manuscript:** The new results section consists of a discussion on the results of each model by each method.

**Referee's comment #47)** L.336-349: "These results emphasize the advantage of high-resolution regional models such as COSMO (~2.5 km resolution) over the IFS global model (resolution of ~13 km in 2015 and ~10 km in 2016) over a diverse area." Although not necessarily surprising, this is one of the few clear results of the paper, and deserves to be discussed and possibly further analyzed. Is the poor performance of the IFS related to lacking representation of the sea breeze circulation or some local scale phenomena?

**Author's response: Comment accepted.**

**Author's changes in manuscript:** An explanation was added to the new summary and conclusions section.

**Referee's comment #48)** Sect. 6.1 and 6.2: Did the authors consider the differences between the bulk Richardson and parcel method, and whether it indicates certain shortcomings in the models description of the boundary layer structure or processes? Comparing the COSMOR and COSMOP mean errors presented in Table 5, it seems that the two methods produce more similar results more inland (Ramat David and Jerusalem) than closer to the coast (Tel Aviv, Beit Dagan, Weizmann). This seems to also hold for the IFS. Is this related to the meteorological conditions, or simply a coincidence? Again, a significantly larger data set would be desirable.

**Author's response: Comment accepted.**

**Author's changes in manuscript:** The new result section consists of a discussion on the differences between the models.

**Referee's comment #49)** Sect. 6.2: Why are only 5 sites included, if ceilometers are available at 8? No station with the description "South" is included in the analysis of spatial variability (Table 1, L. 320), do the included 5 ceilometer sites adequately represent the spatial variability of the studied region?

**Author's response: Comment accepted.**

**Author's changes in manuscript:** The new results section refers to these comments. See response for comment #2.



[Referee's comment #50](#)) L.342-344: "Following the conclusions of previous stages, COSMOR was chosen as the model and method that achieved the best results." In my opinion, this was not well demonstrated (see also comment 46).

[Author's response](#): **Comment accepted.**

[Author's changes in manuscript](#): The new results section includes a discussion of the results by models, methods, and location of the measurement sites.

[Referee's comment #51](#)) L.344: I'm guessing that the time window chosen is somehow related to the diurnal PBL height cycle that was nicely described in Sect. 2. Please provide explanation for the time chosen.

[Author's response](#): **Comment accepted.** In the summer season, stable conditions prevail from sunset to an hour after sunrise (Stull, 1988). At this period the models'  $R_b$  profiles do not accede the relevant thresholds, and the PBL height is not detected. Subsequently, the analysis fixated on the day time hours, after sunrise and before sunset

[Author's changes in manuscript](#): An explanation was added the results section.

[Referee's comment #52](#)) Fig. 4: How are daily values obtained? Is the procedure the same as in Sect. 6.1, e.g. estimating the PBL height at approximately 11 UTC? If so, it should be mentioned in the text.

[Author's response](#): **Comment accepted.**

[Author's changes in manuscript](#): Fig. 4 was replaced by new figures following the referee's recommendations to expand the dataset. See response for comment #2.

[Referee's comment #53](#)) L.349-357: I'm not sure I understand the correction procedure. First, the variables  $\alpha$ ,  $\beta$  and  $\gamma$  are obtained by using the mean error (ME) between model and ceilometer at each station, and the altitude and distance from shoreline as predictor variables. After  $\alpha$ ,  $\beta$  and  $\gamma$  are obtained, it is possible to estimate ME anywhere in the domain. The corrected PBL height is then the COSMOR PBL height+ the ME that is computed using altitude, distance from shoreline and  $\alpha$ ,  $\beta$  and  $\gamma$ . The same procedure is repeated for each hour, resulting in a time dependent  $\alpha$ ,  $\beta$  and  $\gamma$ . Is this a correct interpretation? The authors should clarify the description of their method.

[Author's response](#): **Comment accepted.**

[Author's changes in manuscript](#): The explanation of the correction tool was changed accordingly.

[Referee's comment #54](#)) L.349-357: Could the authors report the values of  $\alpha$ ,  $\beta$  and  $\gamma$ ? The choice of repeating the correction for each hour of the day suggest some dependence of the correction needed on the diurnal cycle, does that exist? Do  $\alpha$ ,  $\beta$  and  $\gamma$  vary from hour to hour? What is the role of  $\gamma$  in the equation, and is it really needed? Presenting  $\alpha$  and  $\beta$  would show whether altitude (e.g. topography) or distance from the shoreline (e.g. sea breeze circulation?) contributes more to the model discrepancy.

[Author's response](#): **Comment accepted.**

[Author's changes in manuscript](#): The new results section provides the dependent variables  $\alpha$ ,  $\beta$ , and the constant  $\gamma$  for each hour (9-14 UTC) for three scenarios: regression by eight ceilometers, regression by seven ceilometers excluding the plain site of Bet Dagan, regression by seven ceilometers excluding the elevated site of Jerusalem.

[Referee's comment #55](#)) L.358: Is the cross-section along a fixed longitude?

[Author's response](#): **Comment accepted.**

[Author's changes in manuscript](#): The new results delineate PBL heights from all ceilometers by distance from the shoreline.

[Referee's comment #56](#)) L.369-370: "The lowest value was corrected from 09 UTC (11 LST) to 14 UTC (16 LST)" - The way I understand this sentence is that the lowest value was before the correction at 9 UTC, and after the correction it was at 14 UTC. This seems to contradict Fig. 5, which shows the opposite. Comparing Figures 5 a and b, it seems that the uncorrected data had the lowest PBL height at 14 UTC (independent of longitude). After the correction, at longitudes eastward of  $35.1^\circ$  (where Jerusalem lies) the lowest PBL height is found at 9 UTC. It would be advisable for the authors to clarify their statement.

[Author's response](#): **Comment accepted.** New figures in the results section clarify the results of the correction tool, hour by hour, from all ceilometer sites.

[Author's changes in manuscript](#): New figures and explanations.

[Referee's comment #57](#)) Line.403: "which improved the description of the diurnal PBL heights" - Unfortunately, there is no evidence presented that the model performance would have improved. See comment 6.

[Author's response](#): **Comment accepted.**

[Author's changes in manuscript](#): The new figures and explanations provide the required evidence.

[Referee's comment #58](#)) Conclusions: The authors could discuss how the results obtained for daytime in a summer month might compare to other seasons.

[Author's response](#): **Comment accepted.** The correction tool is relevant for all dates excluding days with precipitation or dust storms.

[Author's changes in manuscript](#): The comment was added in the new discussion and conclusions Sect.

[Referee's comment #59](#)) Table 1: Height limit is given as 7.7 or 15.4 km, but the footnote states that the data acquisition was limited to 4.5 km. It is not clear what is the vertical extent of the measurement. Although it is not that important for the study, the presentation is confusing and could be clarified.

[Author's response](#): **Comment accepted.** The explanation referred to the difference between the ceilometer's capabilities (hardware) to measure up to 7.7 or 15.4 km, and the actual height ranges of the database. Data acquisition is obtained by the ceilometer's software, which organizes daily profiles up to a specific height limit defined by the user. In our case, the profile height limit was 4.5 km, except for 7.7 in Bet Dagan site.

[Author's changes in manuscript](#): Table 1 was clarified.

[Referee's comment #60](#)) Table 1: The table includes specifications for the sites such as "north", "south", "inland", "mountain", but these do not seem to be defined or used elsewhere in the manuscript. Perhaps the regions could provisionally be indicated on a map, and used in the discussion of the results.

[Author's response](#): **Comment accepted.**

[Author's changes in manuscript](#): A topographical map was added and reference to the regions of each site was included in the results and conclusions sections.

[Referee's comment #61](#)) Table 3: For completeness, the table could include the mean and standard deviation also from the radiosonde used as a reference.

[Author's response](#): **Comment accepted.**

[Author's changes in manuscript](#): The new results section included the mean and standard deviation for six ceilometer sites including radiosonde Bet Dagan.

[Note](#): the comments numbering skip from 61 to 70.

**Referee's comment #70)** Table 4: "The PBL heights were compared to the heights measured by the Beit Dagan ceilometer." The text states (lines 321-322) "the models' results were compared to the ceilometers' measurements in each site". These two statements seem to contradict each other, and I would ask the authors to correct one of them, or to clarify why different comparison measurements are considered in the text and in the table.

**Author's response: Comment accepted.** The clerical error was in the title of the table. Sorry about that.

**Author's changes in manuscript:** The tables and titles were changed.

**Referee's comment #71)** Tables 4 and 5: It would be interesting to also see the mean PBL height of the ceilometer (the reference) at each site.

**Author's response: Comment accepted.**

**Author's changes in manuscript:** The new results section included the mean and standard deviation for 6 ceilometer sites.

**Referee's comment #72)** Figures 1 and 6: Considering the political situation in some areas of Western Asia, the authors should carefully consult the journals guidelines regarding maps.

**Author's response: Comment accepted.**

**Author's changes in manuscript:** The maps were adapted accordingly.

**Referee's comments:**

**Comment #73)** Fig 3a: The figure could contain the PBL height estimated by the two methods. It would be helpful to demonstrate the performance of the two methods.

**Comment #74)** Fig 3b: It does not look like the data has been averaged for 30 min. Is the data presented at original 15 sec resolution? Please clarify in the caption.

**Comment #75)** Fig 3b: The authors should consider showing the time series of ceilometer and model based PBL height in this figure. It would be interesting to see 1) how the wavelet covariance transformation method is performing on the time series presented, 2) how the models predict the temporal development of the PBL height, and 3) whether the difference between model and ceilometer is random or the two models and two methods are consistently over or underestimating the PBL height during this one day. Although it might seem trivial to the authors, this helps the reader to gain confidence in the methods and helps with the understanding of the diurnal cycle of the PBL that is described in Sect.2.

[Comment #76](#)) Fig 3c: The results presented here are not discussed. A description of the results presented here, and the ways they help to interpret Fig. 3 a and b or other results should be added. Furthermore, the wind direction figure could be improved by shifting the x-axis so that it is centered around North (e.g. scale from 180 to 360/0 to 180 degrees).

[Comment #77](#)) Fig 4: Figure 4 is hardly mentioned in the manuscript (it is referred to in the caption of Table 4, and Fig 4b is mentioned on line 326). Consequently, it is not clear what this figure is communicating. What is the additional information provided that is not already presented in Fig. 2? The better performance of COSMO compared to IFS, and the good agreement of ceilometer and radiosonde (Fig. 4b) are already demonstrated in Sect. 6.1.

[Comment #78](#)) Fig. 5: Figure 5 could indicate the locations of the Tel Aviv and Jerusalem ceilometer stations, as well as the mean (and standard deviation) of the PBL height estimated at these sites.

[Comment #79](#)) Fig. 5 and 6: I don't think it is necessary to list the sites and number of days used for the analysis in each figure caption. In my opinion simply a reference to the text for more details would do.

[Comment #80](#)) Fig. 6: Figure 6 could include the information of the mean PBL height at the stations.

[Comment #81](#)) Fig. 6b: It is not clear what variable is presented in Fig 6b. Is it the ME estimated based on Equation 6, or one of the fitted parameters ( $\alpha$ ,  $\beta$ ,  $\gamma$ )?

[Author's response](#):

**Comments accepted.**

[Author's changes in manuscript](#): Fig 1-6 were replaced.

[Referee's comment #82](#)) Citations: The authors should check their citations and list of references list. For example, Uzan et al. (2012) and Uzan et al (2018) are cited but missing from the reference list.

[Author's response](#): **Comment accepted.**

[Author's changes in manuscript](#): Previous citations were checked, and new citations added.

[Referee's comment #83](#)) Figures: The authors should pay attention to the quality of figures. The font size could be increased in almost all figures (especially hard to read is Fig. 3), and use of color-blind friendly colors should be considered.

[Author's response](#): **Comment accepted.**

[Author's changes in manuscript](#): New figures are provided.

# Ceilometers as planetary boundary layer height detectors and a corrective tool for ~~COSMO-ECMWF~~ and ~~COSMO-NWPIFS~~ models

Leenes Uzan<sup>1,2</sup>, Smadar Egert<sup>1</sup>, Pavel Khain<sup>2</sup>, Yoav Levi<sup>2</sup>, Elyakom Vladislavsky<sup>2</sup>, Pinhas Alpert<sup>1</sup>

<sup>1</sup> Porter School of the Environment and Earth Sciences, Raymond and Beverly Sackler Faculty of Exact Sciences, Dept. of Geophysics, Tel-Aviv University, Tel Aviv, 6997801, Israel.  
~~Tel Aviv University, Tel Aviv, 6997801, Israel.~~

<sup>2</sup> The Israeli Meteorological Service, ~~BeitBet~~ Dagan, Israel.

Correspondence to: Leenes Uzan (~~Leenesu@gmail.com~~)(~~Leenesu@gmail.com~~)

## Abstract

The ~~growing importance~~significance of the planetary boundary layer (PBL) height detection is apparent in various fields, ~~from especially in~~ air pollution analysis to weather prediction. ~~Here, we demonstrate the capability of ceilometers to serve as a validation tool for the models' PBL height estimations. The study focused on the daytime summer PBL heights over a heterogeneous area. Height values from two numerical dispersion assessments. Numerical weather models, the global IFS model, produce a high spatial and the regional COSMO model were evaluated against actual measurements from temporal resolution of PBL heights albeit, their performance requires validation. This necessity is addressed here by an array of 8 ceilometers, a radiosonde, and eight two models - IFS global model and COSMO regional model. The ceilometers. The evaluation of the PBL heights was attained by the bulk Richardson method and the parcel method. The ceilometers' backscatter profiles were analyzed by the wavelet covariance transform method. A comparison of the PBL heights at 11 UTC on 33 summer days in Beit Dagan radiosonde launch site revealed a good agreement between the radiosonde, and the adjacent ceilometer (mean error = 12 m, RMSE = 97 m). Spatial analysis on 13 days radiosonde and models by the parcel method and the bulk Richardson method. Good agreement for PBL height was found between the ceilometer and the adjacent Bet Dagan radiosonde (33 m a.s.l) at 11 UTC launching time (N = 91 days, ME = 4 m, RMSE=143 m, R=0.83). The models' estimations were then compared to the ceilometers' results from an additional five ceilometer sites showed COSMO evaluations by the bulk Richardson method (COSMO<sub>R</sub>) produced good results for both flat (mean error = 19 m, RMSE = 203 m) and elevated terrain (mean error = -6 m, RMSE = 251 m). To correct COSMO<sub>R</sub> height estimations, a regression tool was generated based on the PBL height difference between COSMO<sub>R</sub> and~~

34 ~~eight diverse regions where only ceilometers from diverse sites. The independent predictor~~  
~~variables are the topography and the operate.~~ A correction tool was established based on the  
36 ~~altitude (h) and distance from the shoreline. The correction factors are implemented on the~~  
~~COSMO<sub>R</sub> (d) of eight ceilometer sites in various climate regions, from the shoreline of Tel~~  
38 ~~Aviv (h = 5 m a.s.l, d = 0.05 km), to eastern elevated Jerusalem (h = 830 m a.s.l, d = 53 km),~~  
~~and southern arid Hazerim (h = 200 m a.s.l, d = 44 km). The tool examined the COSMO PBL~~  
40 ~~height approximations based on the parcel method. Results for August 14, 2015 case-study,~~  
~~between 9-14 UTC showed the tool decreased the PBL height in the shoreline and inner strip~~  
42 ~~of Israel by ~ 100 m and increased the elevated sites of Jerusalem up to ~ 400 m, and Hazerim~~  
~~up to ~ 600 m. Cross-validation revealed good results without Bet Dagan. However, without~~  
44 ~~measurements from Jerusalem, the tool underestimated Jerusalem's PBL height results up to~~  
~~~600 m difference.~~

46

## 1. Introduction

48 In ~~this~~the era of ~~heavy industrialization~~substantial industrial development, the need to mitigate  
the detrimental effects of air pollution exposure is unquestionable. (~~Anenberg et al., 2019,~~  
50 ~~WHO, 2016, Héroux et al., 2015, Dockery et al., 1993~~). However, ~~in order~~ to regulate and  
establish environmental thresholds, a comprehensive understanding of the air pollution  
52 dispersion processes is necessary. ~~One of the key~~ (Luo et al., 2014, Seidel et al., 2012, Seidel  
~~et al., 2010, Ogawa et al., 1986, Lyons, 1975~~). ~~One of the critical~~ meteorological parameters  
54 governing air pollution dispersion is the planetary boundary layer (PBL) height. (~~Sharf et al.,~~  
~~1993, Garratt, 1992, Ludwing, 1983, Dayan et al., 1988~~). The PBL height is classified as the  
56 first level of the atmosphere ~~which that~~ dictates the vertical dispersion extent of air pollution  
(Stull, 1988). ~~Consequently~~Hence, the ~~concentration level~~quality of air pollution varies  
58 ~~depending on the height~~meteorological data provided to these models is of the PBL. ~~great~~  
importance (Urbanski et al., 2010, Scarino et al., 2014, Su et al., 2018).

60 ~~Applicable evaluation of PBL heights can be derived either by actual measurements or~~  
~~estimations based on numerical~~Numerical weather prediction (NWP) models. ~~On the one hand,~~  
62 ~~NWP models, such as regional models,~~ provide a high temporal and spatial data-resolution  
~~beyond the capability of actual measurements. On the other, they are of PBL height~~ based on  
64 mathematical equations with initial assumptions, and boundary conditioned set beforehand.  
Hence~~However~~, the ~~models' products require a systematic~~ models display difficulty to

66 accurately simulate the PBL creation and evolution (Luo et al., 2014, Seidal et al., 2010), and  
validation ~~tool-based on~~against actual measurements.

68 ~~There are two main PBL height measurement methods: in-~~ is advised. In situ radiosonde  
~~launches and remote sensing such as lidars and profilers. Unfortunately, radiosonde launches~~  
70 ~~are~~atmospheric measurements by radiosondes are most efficient but costly as successive  
measurements. ~~Profilers~~Remote sensing measurements such as wind profilers and  
72 ~~sophisticated lidars produce high temporal resolution profiles but are~~ are mostly designated for  
specific campaigns limited in space. ~~Moreover, certain meteorological conditions may reduce~~  
74 ~~their performance, such as precipitation for radio-acoustic sounding system profilers (Uzan et~~  
~~al., 2012) and dust storms for Raman lidars (location and operational time (Manninen et al.,~~  
76 2018, Mamouri et al., 2016).

~~These limitations have led several research groups to successfully utilized ceilometers—single~~  
78 ~~wavelength cloud base height detectors, as a means to recognize and determine the PBL height~~  
~~(Eresmaa et al., 2006, Haeffelin and Angelini, 2012, Wiegner et al., 2014).~~  
80 UbiquitousCeilometers, on the other hand, are ubiquitous in airports and meteorological  
service centers worldwide, ~~ceilometers obtain a wide spatial resolution per lidar (for further~~  
82 ~~information see (TOPROF of COST Action ES1303 and E-PROFILE of the EUMETNET~~  
Profiling Program). ~~They produce high temporal resolution profiles about every 15 s and every~~  
84 ~~10 m, up to several km, retrieved as attenuated backscatter signals. The ceilometers are low~~  
~~cost, easy to maintain, and operate continuously unattended), thus provide an advantage over~~  
86 the relatively scarce deployment of sophisticated lidars.

Ceilometers are single wavelength micro-lidars intended for cloud base height detection.  
88 Vaisala ceilometers produce backscatter profiles every ~15 s with a vertical resolution of 10 m  
and a height range up to 8 or 15 km, depending on the ceilometer type and the atmospheric  
90 conditions (Uzan et al., 2018). Unlike sophisticated lidars, ceilometers are not equipped to  
provide aerosol properties such as size distribution, scattering, and absorption coefficients  
92 (Ansmann et al., 2011, Papayannis et al., 2008, Ansmann et al., 2003). Nevertheless, their  
advantages have been recognized as low cost, easy to maintain, and continuous unattended  
94 operation under diverse meteorological conditions (Kotthaus and Grimmond, 2018). ~~These~~  
~~qualities reflect their advantages over high-cost, multi-wavelength sophisticated lidars, that~~  
96 ~~require surveillance, calibration procedures,~~Over the years, several studies have assigned  
ceilometers as PBL height detectors (Eresmaa et al., 2006, Van der Kamp and careful



98 maintenance. Hence, they are limited in space and operational time (Mamouri et al., 2016) and  
cannot achieve the spatial and temporal measurements coverage essential to validate the PBL  
100 heights generated by NWP models.

Gierens et al (2018) established a PBL height algorithm applied to the ceilometers' profiles.  
102 The PBL height was classified according to daytime convective mixing and nighttime stable  
surface layer accompanied by a residual layer aloft. Their research was conducted in  
104 northwestern South Africa from October 2012 August McKendry, 2010, Haeffelin and  
Angelini, 2012, Wiegner et al., 2014, showed good agreement with ERA Interim reanalysis.

106 Another operational PBL height detection method was established by Collaud Coen et al.  
(2014). Their study, implemented on a two year data set for two rural sites located on the Swiss  
108 plateau, included several remote sensing instruments (wind profiler, Raman lidar, microwave  
radiometer) and several algorithms (the parcel method, the bulk Richardson number method,  
110 surface based temperature inversion, and aerosol or humidity gradient analysis). The results  
were validated against radio sounding measurements and compared to the NWP model  
112 COSMO 2 (2.2 km resolution). In this research, the authors recommended using ceilometers  
as complementary measurements of the residual layer.

114 Ketterer et al. (2014) focused on the development of the PBL in the Swiss Alps by an adjacent  
ceilometer, wind profiler, and in situ continuous aerosol measurements. The ceilometer's  
116 profiles were analyzed by the gradient and STRAT 2D algorithms. Good agreement was found  
between the PBL height derived from the ceilometer and wind profiler during the daytime and  
118 under cloud free conditions. However, comparisons to the calculated PBL heights from the  
COSMO 2 model yielded low correlations.

120 Despite this extensive research, so far). Previous research employed ceilometers as PBL height  
detectors and compared them to NWP models (Collaud et al., 2014, Ketterer et al., 2014,  
122 Gierens et al., 2018). However, scarce attention has been paid to designate ceilometers asfor a  
correction tool for NWP PBL height assessments. heights. The main goal of this study was to  
124 evaluate the estimations of the models for the daytime summer PBL heights over complex  
terrain by comparing the results against remote sensing measurements from ceilometers.  
126 Ceilometers produce aerosol backscatter profiles, therefore, the evaluation of the PBL height  
during precipitation episodes becomes difficult (is to create this tool and improve the input data  
128 for air pollution dispersion evaluations. A description of the models and instruments applied is

given in ~~Collaud et al., 2014, Ketterer et al., 2014, Kotthaus & Grimmond 2018~~). Accordingly,  
130 ~~this study focused on the summer season.~~

~~The research area and time period are explained in Sect. 2. The models and instruments applied  
132 are described in 2 and Sect. 3 and Sect. 4, respectively. Sect. 4 presents the PBL height  
detection methods are presented. Spatial and temporal analysis of the PBL heights generated  
134 by the models and instruments in six sites are shown in Sect. 5. Results of NWP models  
compared to 1. The PBL height correction tool is explained in situ radiosonde 5.2 and  
136 demonstrated by a case-study employing eight ceilometer measurements are presented in Sect.  
6. Finally, summary sites. Summary and conclusions are drawn in Sect. 7 regarding the  
138 capabilities of NWP models and the evolution of the daytime summer PBL height over Israel.  
6.~~

## **2. Research area**

### **1.1 Study time and region**

142 Located in the East Mediterranean, Israel obtains ~~a heterogeneous research area~~ various climate  
144 measurement sites in comparatively short distances, (Fig. 1). The ceilometer array (Fig. 1,  
Table 1) is comprised of ~~mountains and valleys in the north and the east, a two~~ coastline in the  
146 west and a desert in the south. This provides a range of meteorological conditions, from the  
humid climate on the coast to the arid south.

148 ~~The Israeli summer season (June–September) is characterized by dry weather (no precipitation),~~  
~~high relative humidity (RH) up to 80% in midday in the shoreline (Israeli Meteorological~~  
150 ~~Service–IMS weather reports) and sporadic shallow cumulus clouds. On the synoptic scale,~~  
~~the summer is defined by a persistent Persian Trough (either deep, shallow or medium)~~  
152 ~~followed by a Subtropical High aloft (Felix Y., sites, 40 km apart, in Hadera (10 m a.s.l), and~~  
~~Tel-Aviv (5 m a.s.l). Further inland, 12 km and 23 km southeast to Tel Aviv, are Beit~~ 1994,  
154 Dayan et al., 2002, Alpert et al., 2004). Combined with the sea breeze, the average PBL height  
is found to be quite low. For example, the average summer PBL height in Beit Dagan (33 m  
156 a.s.l and 7.5 km east from the shoreline) reaches ~900 m a.g.l after sunrise, and before the  
entrance of the sea breeze front (Felix) and Weizmann (60 m a.s.l), respectively. About 70 km  
158 southwest to the elevated Jerusalem site (830 m a.s.l) are Hazerim (200 m a.s.l) and Nevatim  
(400 m a.s.l). Ramat David (50 m a.s.l) represents the northern region 24 km inland. ~~Y., 1994,~~

160 ~~Dayan and Rodinzki, 1999, Uzan et al., 2016, Yuval et al., 2019).~~ Summer dust outbreaks in  
the eastern Mediterranean are quite rare (Alpert and Ziv 1989, Alpert et al., 2000) therefore,  
162 they were not addressed here, especially in the height levels below 1 km (Alpert et al., 2002).

Various institutions operate the ceilometers. In several cases, the ceilometers' output files were  
164 not methodically saved. In others, the ceilometers worked for limited periods. Following  
Kotthaus & Grimmond (2018), the analysis concentrated on the dry summer season due to the  
166 difficulty of evaluating the PBL height from backscatter signals during precipitation episodes.  
The database narrowed down by removing dates with partial data or during dust storm events  
168 such as the unprecedented extreme dust storm in September 2015 (Uzan et al., 2018). In  
general, summer dust outbreaks in the eastern Mediterranean are quite rare at the low altitudes  
170 (~ 1-2 km) of the PBL height (Alpert and Ziv 1989, Alpert et al., 2000, Alpert et al., 2002).  
Eventually, the analysis focused the data available from each ceilometer within six summer  
172 months: July-September 2015, and June-August 2016.

A characteristic Israeli summer has no precipitation and mainly sporadic shallow cumulus  
174 clouds (Ziv et al., 2004, Goldreich, 2003, Saaroni and Ziv, 2000). The dominant synoptic  
system is the persistent Persian Trough (either deep, shallow, or medium) followed by a  
176 Subtropical High aloft (Alpert et al., 1990, Feliks Y., 1994, Dayan et al., 2002, Alpert et al.,  
2004). ~~Previous research describes the~~ The average summer PBL height is under 2 km a.s.l  
178 (Dayan et al., 1988, Feliks 2004) Since backscatter signals decline with height, the conditions  
of low PBL heights comes as an advantage.

180

## 1.2 The summer PBL height

182 ~~The formation and evolution of the Israeli summer PBL height are as a function of the synoptic  
and mesoscale conditions, as well as the distance from the shoreline, and the topography.  
184 Overall, the diurnal PBL height in the summer season may be portrayed in the following  
manner follows:~~ After sunrise (~~→~~, ~ 4-5 local standard time (LST, where LST= UTC+2)),  
186 clouds initially formed over the Mediterranean Sea ~~are advected~~, advect eastward to the  
shoreline. As the ground warms up, the nocturnal surface boundary layer (~~SBL~~) dissipates, and  
188 buoyancy induced convective updrafts instigate the formation of the sea breeze circulation  
(Stull, 1988). ~~Previous research of the PBL height in Bet Dagan (33 m a.s.l and 7.5 km east  
190 from the shoreline) revealed an average height of ~900 m a.g.l after sunrise (Koch and Dayan,  
1988, Feliks Y.,1994, Dayan and Rodinzki, 1999, Uzan et al., 2016, Yuval et al., 2019).~~ The

192 ~~entrance of the sea breeze front (SBF) is estimated between 7-9 LST (Felix~~The sea breeze front  
194 enters between 7-9 LST (Felix Y., 1993, Alpert and Rabinovich-Hadar, 2003, Uzan and  
Alpert, 2012), depending on the time of sunrise and the different synoptic modes of the  
prevailing system ~~—~~ the Persian Trough (Alpert et al., 2004). Cool and humid marine air hinder  
196 the convective updrafts. Clouds dissolve, and the height of the shoreline ~~convective~~  
CBL lowers by ~250 m (~~Felix~~Felix Y., 1993, ~~Felix~~Felix Y., 1994, Levi et al., 2011,  
198 Uzan and Alpert, 2012). Further inland, the convective thermals continue to inflate the  
CBL boundary layer (Hashmonay et al., 1991, ~~Felix~~Felix, 1993, Lieman, R. and Alpert, 1993).  
200 ~~The sea breeze circulation steers clockwise and the PBL wind speed is enhanced by the~~  
westWest-north-west synoptic winds enhance the sea breeze wind as it steers north-west  
202 (Neumann, 1952, Neumann, 1977, Uzan and Alpert, 2012). By noontime (~11-13 LST),  
maximum wind speeds further suppress the CBL boundary layer (Uzan and Alpert, 2012). In  
204 the afternoon (~13-14 LST), the ~~SBF~~sea breeze front reaches ~30-50 km inland to the eastern  
elevated complex terrain (Hashmonay et al., 1991, Lieman, R. and Alpert, 1993). At sunset  
206 (~18-19 LST), as the insolation diminishes, the potential energy of the convective updrafts  
weakens, and the CBL boundary layer height drops (Dayan and Rodnizki, 1999). After sunset,  
208 as ground temperature cools down, the ~~CBL~~boundary layer collapses, and a residual  
layer (~~RL~~) is formed above ~~the SBL~~a surface boundary layer (Stull, 1988) ~~as the ground cools~~  
210 ~~down.~~ High humidity and a low ~~RL~~residual layer create low condensation levels, and shallow  
evening clouds are produced.

212

## 2. IFS and COSMO Models

214 ~~The IMS~~ utilizescapitalizes two operational models: The European Centre for Medium-range  
Weather Forecasts (ECMWF) Integrated Forecast System (IFS) global model, and the  
216 ~~consortium~~Consortium for ~~small~~Small-scale ~~modeling~~Modeling (COSMO) regional model.  
~~Details of each model are given in~~ (Table 2).

218 ~~COSMO (~2.5km~~IFS consists of 137 vertical levels. In the years 2015 and 2016 relevant to  
this study, the grid resolution) ~~has been running at the IMS~~ was ~13 km and ~10 km,  
220 respectively. It applies a turbulent diffusion scheme representing the vertical exchange of heat,  
momentum, and moisture through the sub-grid turbulence scale. A first-order K-diffusion  
222 closure based on the Monin-Obukhov (MO) similarity theory represents the surface layer

224 turbulent fluxes. The Eddy-Diffusivity Mass-Flux (EDMF) framework (Koehler et al. 2011)  
describes the unstable conditions above the surface layer.

226 IMS runs COSMO over the Eastern Mediterranean domain (25-39 E/26-36 N) since 2013, with  
228 boundary and initial conditions from IFS. ~~It is based on the primitive~~It consists of 60 vertical  
levels up to 23.5 km and a horizontal grid spacing of 2.5 km (Table 2). Primitive thermo-  
230 hydrodynamic equations ~~describing~~represent the non-hydrostatic compressible flow in a moist  
atmosphere (Steppeler et al., 2003, Doms et al., 2011, Baldauf et al., 2011). ~~Its vertical~~  
~~extension reaches 23.5 km (~30 hPa) with 60 vertical levels.~~The model runs a two-time level  
232 integration scheme, based on a third-order of the Runge-Kutta method, and a fifth-order of  
the upwind scheme for horizontal advection. Unlike ~~IFS, in~~ the ~~deep convection parametrization~~  
~~is switched off, while~~IFS model, in the COSMO model, only ~~the~~ shallow convection is  
234 parameterized, and the deep convection is switched off (Tiedtke, 1989). The turbulence  
scheme, ~~based on of~~ Mellor and Yamada (1982) at ~~Level~~level 2.5, uses a reduced second-order  
236 closure with a prognostic equation for the turbulent kinetic energy. ~~The transport~~Transport and  
local time tendency terms in ~~all the other~~ second-order momentum equations are neglected,  
238 and the vertical turbulent fluxes are derived diagnostically (Cerenzia I., 2017).

~~The resolution of IFS has improved from ~13 km in 2015 to ~10 km in 2016 and consists of~~  
240 ~~137 vertical levels. Its turbulent diffusion scheme represents the vertical exchange of heat,~~  
~~momentum, and moisture through sub-grid scale turbulence. In the surface layer, the turbulence~~  
242 ~~fluxes are computed using a first-order K-diffusion closure based on the Monin-Obukhov (MO)~~  
~~similarity theory. Above the surface layer, a K-diffusion turbulence closure is used everywhere~~  
244 ~~except for unstable boundary layers where an Eddy-Diffusivity Mass-Flux (EDMF) framework~~  
~~is applied to represent the non-local boundary layer eddy fluxes (Koehler et al. 2011).~~

246 ~~The spatial resolution of the~~Both models ~~affects their ability to refer to the actual topography~~  
~~rather than a smoothed grid point. Therefore, the models' results were corrected~~estimate the  
248 PBL height by ~~the actual ground base heights for each measurement site (Table 1).~~

~~Concerning the time resolution,~~The bulk Richardson number method (described in Sect. 4.1).  
250 IFS produced hourly results while COSMO generated profiles every 15 min. ~~To compare PBL~~  
~~heights from both models, a~~ series of trials disclosed ~~that~~the COSMO profiles of the last 15  
252 min within an hour, best represent the hourly values of the IFS model.

254

### 3. Instruments

#### 4.1 Ceilometers

Vaisala ceilometers type CL31, ~~commonly deployed worldwide, are the main~~ is the primary research tool in this study. (Fig.1, Table 1). CL31 is a pulsed, elastic micro-lidar, employing an Indium Gallium Arsenide (InGaAs) laser diode transmitter of ~~a 910 nm ±10 nm~~ near-infrared wavelength ~~of 910 nm ±10 nm~~ at 25°C ~~with~~ and a high pulse repetition rate of 10 kHz, every two seconds (Vaisala ceilometer CL31 user's guide: <http://www.vaisala.com>). The backscatter signals are collected by an avalanche photodiode (APD) receiver and designed as attenuated backscatter profiles at intervals of 2-120 s (determined by the user). ~~In this~~ This study, applied CL31 ceilometers ~~were applied with the exception of~~ except for ceilometer CL51 stationed in ~~the~~ Weizmann Institute (Fig.1, Table 1). CL51 consists of a higher signal and signal-to-noise ratio, ~~hence.~~ Hence the backscatter profile measurement reaches ~~up to ~~~ 15.4 km compared to ~~7~ 8~~ km of CL31. The ceilometers produce 10 m vertical resolution profiles every 15 or 16 sec. Half hourly backscatter profiles improved the signal to noise ratio. The second half-hour profile within each hour defined the hourly profiles.

One drawback is that calibration procedures were nonexistent in all sites, ~~and in.~~ In most cases, maintenance procedures (cleaning of the ceilometer window), were not regularly carried out, ~~with the exception of~~ except for the IMS BeitBet Dagan ceilometer. ~~Nevertheless, the PBL height detection is based on a pronounced change of the attenuated backscatter profile. This change is attributed to variations in the aerosol content providing indications for both clouds and atmospheric layers. Therefore, the limitation of a single wavelength within the spectral range of water vapor absorption does not affect this type of detection. In order to derive the backscatter coefficient from ceilometer measurements~~ In the case of the backscatter coefficients detection, signal calibrations, and water vapor corrections are necessary (Weigner et al., 2014; Wiegner and Gasteiger, 2015).

280

~~The ceilometers produce profiles every 15 or 16 sec (Table 1). In order to compare them to the models' hourly results~~ However, the PBL height detection method employed here (Sect. 4.3), they were averaged to half hour ones, whereas the second half hour profile within each hour was chosen for the comparison process.

284

286 ~~The nocturnal SBL heights in ground level ceilometer sites were detected mainly within the~~  
288 ~~ceilometers' first range gates. At these heights, a constant perturbation existed due to the~~  
290 ~~overlap of the emitted laser beam and the receiver's field of view. This fact limited our~~  
292 ~~capability to determine the low SBL locates the height of the summer season and heightened~~  
~~our decision to focused on daytime CBL heights. Detailed information regarding the~~  
~~manufactural and technical properties of ceilometers involved in this research a pronounced~~  
~~change in the attenuated backscatter profile rather than a specific value. Therefore, calibration~~  
~~procedures are given in Uzannot mandatory (Weigner et al., 2014, Gierens et al., 2018).~~

### 294 **4.2 Radiosonde**

~~The IMS obtains systematic radiosonde atmospheric observations twice daily, at 23 UTC and~~  
296 ~~11 UTC. The radiosonde launching site is adjacent to a ceilometer. Launching is performed~~  
~~in Beit the Bet Dagan ceilometer (32.0 ° long, 34.8 ° lat, 33 m a.s.l), situated, 7.5 km east from~~  
298 ~~the shoreline, 11 km southeast to Tel Aviv, 45 km northwestnorth-west to Jerusalem (, see~~  
300 ~~Fig.1 and Table 1). The radiosonde, type Vaisala RS41-SG, producesretrieves profiles of~~  
~~RHrelative humidity, temperature, pressure, wind speed, and wind direction as it ascends.~~  
302 ~~Measurements are retrieved, every 10 seconds, corresponding to about (~ every 45 m, reaching~~  
~~), rising to ~25 km. Here, we refer to the first 2 km in about 8 minutes. The horizontal~~  
~~displacementfor the detection of the radiosonde depends on the intensity ofmidday summer~~  
304 ~~PBL height. At this height, the ambient wind speed. The average wind speed along theat 11~~  
~~UTC summer profiles is about ~5 m/s (Uzan et al., 2012). Therefore, the horizontal~~  
306 ~~displacement of the radiosonde from its launch position is fairly low and is estimated at aboutis~~  
~~relatively low ~ 2.5 km- and neglected. Moreover, previous research showed the radiosonde~~  
308 ~~position resolution is defined as 0.01°. As aforementioned, the midday PBL height in BeitBet~~  
~~Dagan for midday summer is estimatedis below 1 km (Dayan and Rodinzki, 1999, Uzan et al.,~~  
310 ~~2016, Yuval et al., 2019). Hence, within an ascending height of 1 km, the change in the~~  
~~radiosonde's horizontal position is under), corresponding to horizontal displacement of ~ 0.01°~~  
312 ~~which is an order of magnitude fromwell under the models' grid resolution. Thus, we assert the~~  
~~radiosonde profiles represent the Beit Dagan site and the displacement error of the ascending~~  
314 ~~radiosonde can be neglected. of the IFS and the COSMO models.~~

316

## 54. Methods

### 54.1 The bulk Richardson number method

The COSMO and IFS schemes calculate the PBL height by the bulk Richardson number method ( $R_b$ ) as the most reliable technique for PBL height detection by NWP models (Zhang ~~method~~ et al., 2014).

The bulk Richardson number formula (Hanna R. Steven, 1969, Zhang et al., 2014) is given in the following manner formula below:

$$R_b = \frac{\frac{g}{\theta_v}(\theta_{vz} - \theta_{v0})(Z - Z_0)}{U^2 + V^2} \quad (1)$$

where  $g$  is the gravitational force,  $\theta_{vz}$  is the virtual potential temperature at height  $Z$ ,  $\theta_{v0}$  is the virtual potential temperature at ground level ( $Z_0$ ).  $U$  and  $V$  are the horizontal wind speed components at height  $Z$ . (assuming  $U$  and  $V$  at surface height are insignificant, therefore negligible).

The IFS model defines the PBL height as the lowest height level at which the  $R_b$  (Eq. 1) reaches a critical threshold of 0.25 (ECMWF IFS documentation — Cy43r3, Part IV: Physical Processes, July 2017). The PBL height is distinguished by scanning the bulk Richardson values from the surface level upwards. If the PBL height is found between two levels of the model, it is determined by linear interpolation.

Radiosonde's profiles were analyzed in the same manner by a  $R_b$  threshold of 0.25 to detect a specific height rather than a certain layer.

COSMO estimates the  $R_b$  based on the dynamic conditions of the first four levels (10, 34.2, 67.9, 112.3 m a.g.l.) signified by a threshold of 0.33 for stable conditions and 0.22 for unstable ones. If no level is found, then a missing value is assigned for the PBL height.

The  $R_b$  threshold determines the PBL height. The IFS model has a single limit of 0.25 (Seidel et al., 2012). The COSMO model refers to 0.33 for stable atmospheric conditions (Wetzel, 1982), and 0.22 for unstable conditions by 0.22 (Vogelezang and Holtslag, 1996) in the first four levels of the model (10, 34.2, 67.9, 112.3 m a.g.l.). Linear interpolation determines the height if the detection is between two model levels. The height is assigned with a missing value if the thresholds were not reached. The models' PBL heights ( given as m a.g.l.) are adjusted to the actual altitude of the ceilometer sites (Table 1). The radiosonde 11 UTC PBL heights were



346 defined where the  $R_b$  profile values (derived every 10 sec correspond ding to ~ 45 m) altered  
 348 from negative to positive. In all the dates studied, the first positive value was well above the  
thresholds for unstable conditions by both models (0.25 and 0.33). Therefore the PBL height  
was defined at the height point of the last negative value.

350

#### 4.2 The parcel method

352 ~~The PBL height is defined by the~~The parcel method ~~as defines~~ the PBL height ~~aloft at which~~  
 354 ~~the value of where~~ the virtual potential temperature ~~aloft~~ reaches ~~that of the value evaluated at~~  
 the surface level (Holzworth 1964, Stull, 1988, Seidel et al., 2010). The ~~calculation~~description  
 of the virtual potential temperature is as follows:

$$356 \quad \theta_v = T_v \left( \frac{P_0}{P} \right)^{\frac{R_d}{C_p}} \quad (2)$$

where  $P_0$  is the ground level ~~atmospheric~~ pressure,  $P$  is the ~~at atmospheric~~ pressure at height  
 358  $Z$ ,  $R_d$  is the dry air gas constant ~~of dry air~~,  $C_p$  is the heat capacity of dry air ~~in a constant~~  
~~pressure~~ ( $\frac{R_d}{C_p} = 0.286$ ). The virtual temperature ( $T_v$ ) is obtained by:

$$360 \quad T_v = \frac{T}{1 - \frac{e}{P}(1 - \varepsilon)} \quad (3)$$

where  $T$  is the temperature at height  $Z$ ,  $e$  is the actual vapor pressure, and  $\varepsilon$  is the ratio of ~~the~~  
 362 ~~gas constant~~molecular weight of ~~air and~~ water vapor and dry air ( $\varepsilon = 0.622$ ). ~~The actual vapor~~  
~~pressure ( $e$ ) is derived by the relative humidity (RH) profile multiplied by the saturated vapor~~  
 364 ~~pressure ( $e_s$ ). The saturated vapor pressure was derived by the temperature profile.~~

~~In this method, the value of the~~The virtual potential temperature ~~at surface height is crucial.~~  
 366 ~~The first levels of IFS profiles were computed based on the available meteorological~~  
~~parameters from the models and COSMO are 10 m a.g.l. radiosonde: mixing ratio, pressure,~~  
 368 ~~and 20 m a.g.l, respectively. Thus, evaluations of the ambient temperature and the profiles~~  
~~from the IFS model. Relative humidity, pressure, and temperature profiles from the COSMO~~  
 370 ~~model and the radiosonde. The virtual potential temperature profiles of the models at ground~~  
~~level were obtained by the temperature and dew point temperature (or RH) for at 2 m a.g.l are~~  
 372 ~~generated by the models based on the.~~ These parameters were derived from the models by the

similarity theory. Finally, the PBL heights (given in m. a.s.l) were adjusted to the actual altitude of the ceilometer sites (Table 1).

374

### 376 **5.4.3 The wavelet covariance transform method**

The wavelet covariance transform (WCT) method ~~is operated along the length of the backscatter profile (Baars et al., 2008, Brooks Ian, 2003). This method~~ is based implemented on backscatter profiles by the Haar step function (Baars et al., 2012) formula given in Eq. (4) ~~and Eq. (5) as follows~~:

378  
380

$$W_{f(a,b)} = \frac{1}{a} \int_{Zb}^{Zt} f(z) h\left(\frac{z-b}{a}\right) dz \quad (4)$$

382

where  $W_{f(a,b)}$  is the local maximum of the backscatter profile ( $f(z)$ ) determined within the range of step ( $a$ ) ~~by the Haar step function ( $h$ ).~~ The length of the step is the number of height levels ( $n$ ) multiplied by the profile height resolution ( $\Delta z$ ) from ground level ( $Zb$ ) and up ( $Zt$ ). In this study,  $Zb$  was defined as the height above the perturbation of the overlap function ( $\sim 100$  m), and  $Zt$  as the height with the most significant signal variance or, the first appearance of negative values. Both thresholds indicate a low signal-to-noise ratio.  $Zb$  is the lowest height among the two options. These thresholds apply under clear sky conditions. When clouds exist in the summer, they are mainly shallow cumulus clouds (Sect. 1.1). The PBL height is the height within the cloud, above the cloud base height (Wang et al. 2012, Stull 1988).

384

386

388

390

The Haar step function, ~~given in Eq. (5), (4)~~ is equivalent to a derivative at height  $z$ , representing the value difference of each step ( $a$ ) above and beneath a point of interest ( $b$ ). Here In this study,  $b$  is the measurement heights of the ceilometer along the backscatter profile (every 10 m starting from 10 m a.g.l) and . The value of the step  $a$  was defined as 20 m (10 m above and beneath point  $b$ ). ( $a$ ) varied for each ceilometer, depending on the site location.

392

394

396

$$h\left(\frac{z-b}{a}\right) = \begin{cases} +1, & b - \frac{a}{2} \leq z \leq b, \\ -1, & b \leq z \leq b + \frac{a}{2} \\ 0, & \text{elsewhere} \end{cases} \quad (5)$$

398

~~To evaluate the ceilometers' PBL heights (Eq. 4), the backscatter profiles are analyzed by the WCT method between two boundaries. The lower boundary ( $Zb$ ) is the height above the~~

400 ~~perturbation of the overlap function (~100 m, see Sect. 4.1). The upper limit ( $Z_t$ ) is either the~~  
~~height point with the largest variance within a step or the first height point with negative values~~  
402 ~~indicating a low signal to noise ratio. The lowest height among the two aforementioned options~~  
~~will define the upper limit.~~

404 ~~When clouds exist (mainly shallow cumulus clouds), the algorithm defines the PBL height as~~  
~~the highest measurement point of the cloud above the cloud base height. This height indicates~~  
406 ~~the entrainment zone rather than the actual cloud top.~~

408 ~~6In arid and dusty areas such as Nevatim and Hazerim, specifically on clear days, the WCT~~  
~~method failed to distinguish the PBL height (Van der Kamp and McKendry, 2010, Gierens et~~  
410 ~~al., 2018). The analysis excluded these cases. The last stage consisted of manual inspection of~~  
~~the WCT results.~~

412

## **5. Results**

414 ~~In the Israeli summer season, stable PBL conditions are generated from sunset to an hour after~~  
~~sunrise (Stull, 1988). At this period the models'  $R_b$  profiles do not accede the relevant~~  
416 ~~thresholds, and a missing value is assigned (Sect. 4.1). Additionally, the difficulty to estimate~~  
~~the surface boundary layer by ceilometers (Gierens et al., 2018) was associated with a constant~~  
418 ~~perturbation within the first range gates due to the overlap of the emitted laser beam and the~~  
~~receiver's field of view (Weigner et al., 2014). **6.1 Comparison to in-situ radiosonde profiles**~~

420 ~~In order to evaluate the daytime PBL heights produced by the models and the ceilometers,~~  
~~Hence, the analysis focused on the midday summer PBL heights.~~

422

### **5.1 Spatial and temporal analysis**

424 ~~The analysis was performed based on six ceilometers with available data of at least 50 days~~  
~~within the study period: Bet Dagan, Tel Aviv, Ramat David, Weizmann, Jerusalem, and~~  
426 ~~Nevatim. In Bet Dagan, the results were compared to the radiosonde's evaluations.~~  
~~Consequently, the investigation was held in Beit Dagan launch site at the time of the midday~~  
428 ~~launch (11 UTC). For this comparison, the ceilometer's 15 s profiles were averaged as half-~~  
~~hour profiles between 10:30-11:00 UTC. COSMO's results referred to the profiles of 10:45~~

430 UTC, and IFS estimations were given radiosonde, thereupon, the analysis fixated at 11 UTC.  
The analysis was carried out launching time. In the remaining five sites, the models compared  
432 to the ceilometers. Statistical analysis for 33 summer days, 13 days from August 2015, and 20  
days from Aug 2016. The PBL heights were produced by the same methods: the parcel method  
434 (denoted by subscript P) and the bulk Richardson method (denoted by subscript R). These  
methods require meteorological parameters such as temperature and pressure profiles  
436 generated by the models and the radiosonde. Ceilometers, on the other hand, produce only  
backscatter signals. Therefore, they were analyzed by the WCT method. The results were  
438 statistically analyzed by each site presents the mean error (ME), root mean square error  
(RMSE), and correlation (R) presented in Fig. 2 and Table 3., Mean and standard deviation  
440 (STD) given in tables and plots.

Good agreement was found between the ceilometer and the radiosonde (RS) in Bet Dagan (Fig.  
442 2 and Table 3, ME = 12 m, RMSE = 97 m, and R = 0.93), although they produced 143, R =  
0.83). The IFS by the parcel method (IFS-pm) appears to overestimate the PBL heights by  
444 different methods height (ME = 346, RMSE = 494, R = 0.14), as well as by the Richardson  
method (IFS-ri, ME = 366, RMSE = 579, R = -0.13). Among the models and methods,  
446 COSMO<sub>R</sub> retrieved the COSMO model by the parcel method derived the best results of ME =  
-3 m, RMSE = 152 m and R = 0.83). IFS predominantly overestimated the PBL heights. The  
448 poorest results were generated by IFS<sub>R</sub> (ME = 274 m, RMSE = 432 m, R = 0.18) (COSMO-pm,  
ME = -52, RMSE = 146, R = 0.84).

450 In the shoreline site of Tel Aviv (Fig. 3, Table 4), COSMO-pm displayed good agreement with  
the ceilometer measurements (ME = 17, RMSE = 183, R = 0.74), similar to COSMO-ri (ME  
452 = 18, RMSE = 187, R = 0.7). IFS-ri produced the highest overestimations (ME = 436, RMSE  
= 616, R = -0.03).

454 In Ramat David, stationed in the northern inner plain of Israel, the parcel method derived better  
results than the Richardson method in both models (Fig. 4, Table 5). Among the models,  
456 COSMO displayed better results (ME = 40, RMSE = 245, R = 0.55). IFS-ri generated the  
poorest correlation (ME = 446, RMSE = 745, R = -0.08).

458 In Weizmann (Fig. 5 Table 6), 11 km southeast to Bet Dagan, IFS-ri produced the poor results  
(ME = 430, RMSE = 604, R = -0.01), conversley to the good results by the parcel method (ME  
460 = 67, RMSE = 162, R = 0.85). The COSMO model derived similar results by both methods  
(COSMO-pm: ME = -106, RMSE = 207, R = 0.76, COSMO-ri: ME = 21, RMSE = 192, R =  
462 0.72).

464 In the mountainous site of Jerusalem, the bulk Richardson method produced better results than the parcel method in both models (Fig. 6, Table 7). COSMO-pm derived good results (ME = -44, RMSE = 239, R = 0.70) and IFS-ri the poorest (ME = 366, RMSE = 498, R = 0.18).

466 In the elevated and arid site of Nevatim, overall correlations were weak (0.1-0.3) and high RMSE (369 - 488).

468 Main conclusions derived from Fig.2-7 are summarized below:

- 470 - Low correlation in Nevatim (0.1-0.3) demonstrates the difficulty of the models to assess the PBL height over complex terrain. Evaluation of PBL heights in complex terrain was studies by Ketterer et al. (2014) in the Swiss Alps by a ceilometer, wind profiler, and in-situ continuous aerosol measurements. The ceilometers analyzed by the gradient and STRAT-2D algorithms and the wind profiler by the range-corrected SNR method. The results compared to the COSMO-2 regional model. The results showed good agreement found between the heights derived by the ceilometer and wind profiler during the daytime cloud-free conditions ( $R^2=0.81$ ). However, in most cases, the model underestimated the PBL height. The researchers presumed the grid resolution, parametrization schemes, and the surface type did not match the real topography. The comparison between a single measurement point and a grid point is not straight forward.
- 480 - The parcel method achieved better results in Ramat David, Tel Aviv, Bet Dagan, and Weizmann. In the elevated site of Jerusalem, the correlation of COSMO-ri was the highest (R=0.7).
- 484 - The COSMO model produced better results in the shoreline and plain regions (Ramat David, Tel Aviv, Bet Dagan) except for Weizmann (60 m a.s.l, 11.5 km from the coastline), where IFS-pm obtained the highest correlation (R=0.85).

486 IFS model based on the bulk Richardson method overestimated the PBL heights ( ~ 420 m) in the plain sites of Bet Dagan, Tel Aviv, Weizmann, and Ramat David. The bulk Richardson evaluation (See Sect. 4.1) includes the horizontal wind speed profiles that are less accurate and may contribute to the discrepancies. Collaud et al. An example of an analysis on a typical day is given in Fig. 3 for August 15, 2015. On this day, the PBL height at 11 UTC was estimated at 680 m a.s.l by the radiosonde. COSMO<sub>P</sub> accurately estimated the same height while COSMO<sub>R</sub> detected the height to be 100 m lower (580 m a.s.l). The ceilometer overestimated by 100 m (795 m a.s.l). IFS results were twice the value produced by the radiosonde (IFS<sub>R</sub>=1,300 m a.s.l, IFS<sub>P</sub>= 1,474 m a.s.l).

Among the 33 days tested, the largest gap was found between IFS<sub>R</sub> and RS<sub>R</sub> on August 17, 2016 (Fig. 2). The imprecision could be due to the fact that the Richardson method is based solely on dry thermodynamics for local turbulence (Von Engeln and Teixeira, 2013), while on August 17, 2016, the 11 UTC PBL height was determined through a multi-layer cloud (not shown).

## 6.2 Spatial analysis by ceilometers

After the good results generated by the WCT method imposed on the ceilometer's profiles, ceilometers were applied as PBL height detectors in sited where no other atmospheric measurements operated. The same analysis process was carried out but for five ceilometer sites (Ramat David, Tel Aviv, Beit Dagan, Weizmann, and Jerusalem), representing diverse terrain on 13 specific days available from all instruments and models. This time the models' results were compared to the ceilometers' measurements in each site. Both models defined the Tel Aviv site by a grid point mostly over the Mediterranean Sea. Therefore, we shifted the Tel Aviv coordinates to an adjacent grid point that was mostly land, representing Tel Aviv by the same height and distance from the shoreline.

A comparison to radiosonde's results was available only in Beit Dagan. Figure 4b reveals a good agreement between the radiosonde and the ceilometer's evaluations in Beit Dagan, although the different methods imposed on each instrument. A significant case on August 10, 2015, where an atmospheric layer above the PBL height denoted by the radiosonde and the ceilometer (not shown) led to the models' discrepancies.

By and large, COSMO<sub>R</sub> achieved the best statistical results (Tables 4-5) regarding flat and complex terrain, of RMSE from 175 m in Weizmann (60 m a.s.l, and 11.5 km east from the shoreline) up to 251 m in Jerusalem (830 m a.s.l and 53 km east from the shoreline), and ME between 19 m in Tel Aviv (5 m a.s.l, and 50 m from shoreline), and 26 m in Ramat David (50 m a.s.l, and 24 km east from the shoreline). IFS<sub>P</sub> produced high RMSE results starting at 180 m in Ramat David rising up to 569 m in Beit Dagan, and ME up to 497 m in Beit Dagan. These results emphasize the advantage of high-resolution regional models such as COSMO (~2.5 km resolution) over the IFS global model (resolution of ~13 km in 2015 and ~10 km in 2016) over a diverse area.

6.3 (2014) referred to the limitations of the bulk Richardson method of the COSMO-2 regional model (2.2 km resolution), which overestimated the convective boundary layer

by 500–1000m. They explained the Richardson method is sensitive to the surface temperature, and errors and uncertainties in the model's temperature and relative humidity profiles could explain the significant bias. Also, the occurrence of clouds, which may be missing in the model, can lead to lower PBL heights.

## 5.2 COSMO PBL height correction

Finally, the spatial daytime summer PBL heights were investigated. Following the conclusions of previous stages, COSMO<sub>R</sub> was chosen as the model and method that achieved the best results. Average hourly values were derived between 09–14 UTC (corresponding to 11–16 LST) and compared to the results from eight ceilometer sites (Fig. 1, Table 1). The comparison was accomplished by all dates available for each ceilometer site on August 2015: Jerusalem—21 days, Nevatim—13 days, Hazerim—20 days, Ramat David—26 days, Weizmann—25 days, Beit Dagan—13 days, Hadera—16 days, Tel Aviv—25 days.

In order to validate and correct COSMO<sub>R</sub> results by the ceilometers' measurements, a correction tool based on a regression function was implemented for each hour (09–14 UTC), for all ceilometers' sites simultaneously by the following formula:

A correction formula for the models' PBL height employing ceilometers is given below:

$$dH_{st} = \alpha G + \beta D + \alpha h_{st} + \beta d_{st} + \gamma \quad (6)$$

where  $ME_{st}$  is the dependent variable representing the PBL height mean error for each ceilometer station (st) compared to the results obtained by the COSMO<sub>R</sub>. The independent predictor variables are the ground altitude of the ceilometer's site (G) and its distance from the shoreline (D). The correction factors  $\alpha$ ,  $\beta$ , and  $\gamma$  are implemented on the COSMO<sub>R</sub> PBL height results.

COSMO<sub>R</sub> mean PBL heights cross-section from Tel Aviv (34.8° lat) to Jerusalem (35.2° lat) is presented in Fig. 5. Before the correction (Fig. 5a), COSMO<sub>R</sub> approximated Tel Aviv PBL heights descend gradually from 750 at 09 UTC (11 LST) to 600 m a.s.l at 14 UTC (16 LST). Apparently, the correction tool reduced the height difference to ~700 m a.s.l with the exception of ~750 m a.s.l at 09 UTC (Fig. 5b). These results correspond to Uzan et al, (2012) showing

556 ~~Tel Aviv site is practically on the shoreline, therefore as the sea breeze enters Tel Aviv (~08 UTC), it surmounts the convective thermals preventing from the mixed layer to inflate.~~

558 ~~In Jerusalem, the summer PBL height inflates according to the insolation intensity, as the main source of the buoyancy force. Therefore, the maximum daytime PBL heights are measured at~~  
560 ~~midday. In the afternoon, when the sea breeze reaches eastern Israel, the height decreases. COSMO<sub>R</sub> results before and after the correction showed the highest value at 11 UTC (13 LST),~~  
562 ~~corresponding to maximum insolation at midday. The lowest value was corrected from 09 UTC (11 LST) to 14 UTC (16 LST) as insolation decreases and the cool and humid air of sea~~  
564 ~~breeze front demolishes the thermals and the PBL height subsides.~~

~~Between the shoreline of Tel Aviv and the eastern mountains of Jerusalem, the overall range~~  
566 ~~of PBL height values was reduced. For example, in 35° lat (between Weizmann 60 m a.s.l and Jerusalem 830 m a.s.l), the PBL heights of 09-14 UTC varied from 750 to 1500 m a.s.l.~~  
568 ~~After the correction, the height values ranged from 1000 to 1400 m a.s.l, generating higher PBL heights for the daytime hours. Fig. 6 demonstrated the correction tool at 14 UTC~~  
570 ~~disclosing a correction of ~300 m (Fig. 6b) over the complex terrain of Jerusalem (830 m a.s.l) and Nevatim (400 m a.s.l).~~

572

7Where  $dH_{st}$  is the PBL height difference between the ceilometer and the model, the altitude  
574 ( $h_{st}$ ), and distance from the shoreline ( $d_{st}$ ) for each measurement site ( $st$ ). The formula runs  
simultaneously for all ceilometer sites to derive the dependent variables  $\alpha$ ,  $\beta$ , and the constant  
576  $\gamma$ . The formula is suitable for both models

A case-study demonstrates the correction formula on August 14, 2015, from the COSMO  
578 model based on the parcel method (COSMO-pm). COSMO-pm is the model and method that  
derived good results in Sect. 5.1. The formula runs for each hour between 9-14 UTC for the  
580 daytime PBL height (See Sect. 5). Results are portrayed for each hour by a 2-D plot of the  
height correction within the area of ceilometers' deployment. Along with an east-west cross-  
582 section plot, corresponding to the location of the ceilometers. Cross-validation tests for Bet  
Dagan and Jerusalem show the effectivity of the correction formula. Main findings for each  
584 hour are as follows:

9 UTC (Fig. 8): Along the coast, the correction tool lowers the PBL height by 70 m to 670 m  
586 and increases by 90 m in the inner strip of Israel to ~ 890 m a.s.l. Cross-validation for Bet



588 Dagan (CV-BD) shows good results, whereas, in Jerusalem (CV-JRM), the correction tool  
reduced the height by 600 m.

590 10 UTC (Fig. 9): The correction tool distinguishes between the coastal sites of Tel Aviv and  
Hadera, and the inland locations of Bet Dagan and Weizmann, only ~ 10 km apart from Tel  
592 Aviv. While the correction tool increased the height of the coastal stations, a slight height  
decreased was performed in the inner sites. In the arid southern Hazerim, the correction tool  
594 lowered the PBL height by 400 m. In the desert south of Nevatim, the correction tool decreased  
the PBL height by 200 m. Cross-validation of Jerusalem (CV-JRM) underestimates the PBL  
height in Jerusalem by 400 m.

596 11 UTC (Fig. 10): A distinction between the shoreline and the inner sites is more evident, as  
the PBL height of Tel Aviv and Hadera is increased by ~100 m to ~700 m a.s.l, whereas, Bet  
598 Dagan and Weizmann remained ~ 800 m a.s.l. This finding corresponds to Uzan et al. (2016)  
analysis of the mean diurnal-cycle of the PBL height from July to August 2014, based on  
600 ceilometer measurements. A pronounced correction is visible in the elevated southern site of  
Hazerim by 550 m down to 1120 m a.s.l. This gap is not unexpected since NWP models have  
602 difficulty assessing the meteorological conditions over complex terrain. Here, Jerusalem cross-  
validation (CV-JRM) underestimates the PBL height by a comparatively lower range of 200  
604 m.

606 12 UTC (Fig. 11): The correction tool increased the PBL height in the coast and inland stations,  
but in fact, the height is lower than an hour before. The PBL height in Hazerim is decreased by  
300 m. Jerusalem cross-validation (CV-JRM) underestimates the PBL height in Jerusalem by  
608 600 m.

610 13 UTC (Fig. 12): The correction tool increased the PBL heights. A substantial increase of 380  
m in Jerusalem generates a height of ~1750 m a.s.l. Jerusalem cross-validation (CV-JRM)  
underestimates the PBL height by 550 m.

612 14 UTC (Fig. 13): Similar to an hour before, the correction increases the PBL height in all sites,  
but in fact, the PBL heights are lower than an hour earlier, except a mild increase in the coastal  
614 locations of Tel Aviv and Hadera. Jerusalem cross-validation (CV-JRM) underestimates the  
PBL height by ~300 m.

616

618 **6. Summary and Conclusions**

620 The primary purpose of this study was to improve the performance of air pollution dispersion  
models by providing applicable data of PBL heights from NWP models employing ceilometers.  
622 A correction tool using ceilometer measurements was established to validate the models' PBL  
height assessments. The study focused on the summer PBL heights (July-September 2015,  
June-August 2016) during the day hours (9-14 UTC). At this period, the highest air pollution  
624 events occur in Israel from tall stacks (Dayan et al., 1988, Uzan et al., 2012).

The study contained eight ceilometers, a radiosonde, two models - IFS and COSMO, and three  
626 PBL height analysis methods. The bulk Richardson method, the parcel method for the models  
and radiosonde, and the WCT method for the ceilometers. In Bet Dagan radiosonde launching  
628 site, results revealed good agreement between the ceilometer's PBL heights and the radiosonde  
(N = 91 days, ME = 4 m, RMSE=143 m, R=0.83). In Ramat David, Tel Aviv, Weizmann,  
630 Jerusalem, and Nevatim, the models were compared to the ceilometers. The COSMO model  
performed better in the plain areas of Tel Aviv (10 m a.s.l), Bet Dagan (33 m a.s.l), and Ramat  
632 David (50 m a.s.l) and the mountainous Jerusalem (830 m a.s.l). The IFS model showed good  
agreement with the ceilometer in Weizmann (60 m a.s.l, N=55 days, ME = 67 m, RMSE = 162  
634 m, R=0.85). In the arid southern site of Nevatim (400 m a.s.l), overall correlations were poor.  
The IFS-pm produced better in Bet Dagan, Ramat David, Tel Aviv, and Weizmann (four out  
636 of five sites except for Nevatim). The COSMO-pm produced better results in Bet Dagan and  
Ramat David, while in Tel Aviv the results generated by both methods were similar (N = 123  
638 days, COSMO-pm: ME = 17 m, RMSE = 183 m, R=0.74, COSMO-ri: ME = 18 m, RMSE =  
180 m, R=0.80).

640 The PBL height correction tool for the NWP models is based on the altitude and the distance  
from the shoreline of the ceilometers' measurement sites. A case-study demonstrated the tool's  
642 feasibility on August 14, 2015. Moving from 9 to 14 UTC, the correction decreased the PBL  
height in flat terrain (Tel Aviv, Hadera, Bet Dagan, and Ramat David). This finding  
644 corresponds with Uzan et al., 2016, analyzing the diurnal PBL height of Bet Dagan and Tel  
Aviv in the summer of 2014. Similar results produced in Hadera describe the summer PBL  
646 height between 1997-1999 and 2002-2005 based on measurements from a wind profiler (Uzan  
et al., 2012). Koch and Dayan (1992) revealed air pollution episodes of sulfur dioxide increased  
648 in shallow PBL heights in the coastal plain of Israel. Uzan et al. (2012) showed an average

decrease of ~ 100 m in the coastal PBL height resulted in an average increase of ~200 air pollution episodes of sulfur dioxide.

The tool increased the PBL height in the elevated site of Jerusalem (830 m a.s.l) by ~380 m. In the arid south in Hazerim (200 m a.s.l), the tool lowered the PBL height by ~ 550 m. The significant height corrections in the elevated sites are attributed to the models' difficulty to imitate local meteorological processes in complex terrain (e.g., Alpert et al., 1984). Dayan et al. (1988) presumed the diurnal cycle and the prevailing synoptic systems govern the temporal behavior of the Israeli summer PBL height. The strength of the sea breeze determines significant variations in the inner PBL heights.

Cross-validation for Bet Dagan produced excellent results. Bet Dagan is located in flat terrain 11 km north to the Weizmann site and 12 km southeast to Tel Aviv site. Without the single measurement site in Jerusalem (830 m a.s.l), the correction tool failed to generate Jerusalem's PBL height and produced lower values up to a 600 m difference. This finding shows the process of cross-validation can assist in defining the required ceilometers' deployment in the future.

#### ~~In summary, Summary and Conclusions~~

~~Earlier studies have successfully employed ceilometers for PBL height detection, typically under dry conditions. However, these studies employed weather models primarily as a validation tool rather than investigating the models' predictive capabilities. Here, we tested the ability of ceilometers to serve as a correction tool for PBL height estimations derived from two operational models: the IFS global model, and the mesoscale COSMO regional model. The study focused on the daytime summer PBL heights.~~

~~Firstly, we compared the models' and the ceilometer's evaluations to actual measurements from an adjacent radiosonde in the Beit Dagan launch site. Results for 11 UTC on 33 August days revealed the promising ability of the WCT method to detect the PBL heights generated by the radiosonde by the bulk Richardson method and by the parcel method (RMSE=97 m).~~

~~In the next stage, the investigation expanded spatially to four other diverse measuring sites, from the shoreline of Tel Aviv (5 m a.s.l) to the mountainous Jerusalem (830 m a.s.l). The same methods were applied for 13 summer days, except this time, the models' values were compared to the ceilometers' measurements in each site. The results disclosed the COSMO model based on the bulk Richardson method (COSMO<sub>R</sub>) achieved the best results for both flat (Tel Aviv: RMSE=203 m, ME=19 m) and complex terrain (Jerusalem: RMSE=251m, ME=-6 m).~~

680 ~~Finally, the temporal and spatial evolution of the summer daytime (11–16 LST) PBL heights~~  
681 ~~were examined. The heights were derived by COSMO<sub>R</sub> and compared to ceilometers~~  
682 ~~measurements distributed in eight sites across Israel, providing a heterogeneous research area~~  
683 ~~in comparatively short distances. A correction tool was established based on a regression~~  
684 ~~function comprised of the topography of the ceilometer's site (G) and its distance from the~~  
685 ~~shoreline (D) serving as the independent predictor variables. The results revealed corrections~~  
686 ~~up to ~300 m difference which improved the description of the diurnal PBL heights.~~

~~Despite the limited database,~~ our results offer a preview of the great potential of ceilometers as  
687 a ~~validation and a~~ correction tool ~~to discern for~~ PBL heights derived from ~~weather~~NWP models.  
688 ~~This tool demonstrates the benefit of deploying ceilometers, specifically in complex terrain.~~  
689 Future research should, ~~therefore,~~ include a larger dataset to ~~evaluate whether these results are~~  
690 ~~retained in the long term and to define~~ create a systematic ~~validation process.~~ correction process  
691 and produce sufficient input data for mandatory air pollution dispersion assessments.

#### 694 ~~-~~ **Data availability**

Weather reports - Israeli Meteorological Service weather reports (in Hebrew):  
695 <http://www.ims.gov.il/IMS/CLIMATE/ClimateSummary>.  
Radiosonde profiles - Israeli Meteorological Service provided by request.  
696 Ceilometer profiles - the data is owned by ~~governmental offices~~ several institutions and  
697 provided by request.

700

#### **Author contribution**

701 Leenes Uzan carried out the research and prepared the manuscript under the careful guidance  
702 of Pinhas Alpert and Smadar Egert alongside a fruitful collaboration with Yoav Levi, Pavel  
703 Khain, and Elyakom Vladislavsky. The authors declare that they have no conflict of interest.

#### 706 **Acknowledgments**

We wish to thank the Israeli Meteorological Service, the Israeli Air Force, the Association of  
707 Towns for Environmental Protection (Sharon-Carmel), and Rafat Qubaj from the Department  
708 of Earth and Planetary Sciences at the Weizmann Institute of Science, for their ceilometer data.  
709 We ~~are indebted to Hadas Mareu~~ thank Noam Halfon from the IMS for ~~her editing assistance.~~  
710 the topography map

712 **References**

714 Alpert, P. and J. Neumann, On the enhanced smoothing over topography in some mesometeorological models, Bound. Lay. Met., 30, 293-312, 1984.

Alpert P., and Ziv B.: The Sharav cyclone observations and some theoretical considerations, J. Geophys. Res., 94, 18495–18514, 1989.

718 Alpert, P., Abramsky, R., Neeman, B.U.: The prevailing summer synoptic system in Israel- Subtropical high, not Persian Trough, Isr. J. Earth Sci, 39, 93-102, 1990.

720 Alpert P., Herman J., Kaufman Y. J., and Carmona I.: Response of the climatic temperature to dust forcing, inferred from TOMS Aerosol Index and the NASA assimilation model. J. Atmos. Res., 53, 3-14, 2000.

722 Alpert, P., Krichak, S. O., Tsidulko, M., Shafir, H., and Joseph, J. H.: A Dust Prediction System with TOMS Initialization, Mon. Weather Rev., 130, 2335–2345, 2002.

724 Alpert P., and Rabinovich-Hadar M.: Pre- and post-frontal lines - A meso gamma scale analysis over south Israel, J. Atmos. Sci., 60, 2994-3008, 2003.

726 Alpert, P., Osetinsky, I., Ziv, B., Shafir H.: Semi-objective classification for daily synoptic systems: Application to the eastern Mediterranean climate change. Int. J. of Climatol., 24, 728 1001-1011, 2004.

730 Anenberg, S., Miller, J., Henze, D., & Minjares, R.: A global snapshot of the air pollution-related health impacts of transportation sector emissions in 2010 and 2015. ICCT report, Washington, D.C., 2019.

732 Ansmann et al.: Long-range transport of Saharan dust to northern Europe: The 11–16 October 2001 outbreak observed with EARLINET, J. of Geo. Phys. Research, 108, D24, 4783, 734 doi:10.1029/2003JD003757, 2003.

736 Ansmann, A., Petzold, A., Kandler, K., Tegen, I.N.A., Wendisch, M., Mueller, D., Weinzierl, B., Mueller, T. and Heintzenberg, J.: Saharan Mineral Dust Experiments SAMUM–1 and SAMUM–2: what have we learned? Tellus B, 63(4), 403-429, 2011.

738 Baars, H., Ansmann, A., Engelmann, R., and Althausen, D.: Continuous monitoring of the boundary layer top with lidar, Atmos. Chem. Phys., 8, 7281–7296, https:// doi:10.5194/acp-8- 740 7281-2008, 2008.

Baldauf, M., A. Seifert, J. Förstner, D. Majewski, M. Raschendorfer, and T. Reinhardt:  
742 Operational Convective-Scale Numerical Weather Prediction with the COSMO Model:  
Description and Sensitivities. Mon. Wea. Rev., 139, 3887–3905,  
744 <https://doi.org/10.1175/MWR-D-10-05013.1>, ~~2004~~2011.

~~Bechtold~~Bechthold, P.: Convection parametrization. ECMWF Seminar proceedings on “”The  
746 parametrization of subgrid physical processes””, 63-85, 2008.

Briggs, G.A.: Plume rise predictions. In: Haugen, D.A. (Ed.), Lectures on Air Pollution and  
748 Environmental Impact Analysis, American Meteorological Society,  
pp. 59–111, 1975.

750 Brooks, I.: Finding Boundary Layer Top: Application of a wavelet covariance transform to  
lidar backscatter profiles, J. Atmos. Ocean. Tech., 20, 1092–1105, 2003.

752 Cerenzia I., Challenges and critical aspects in stable boundary layer representation in numerical  
weather prediction modeling: diagnostic analyses and proposals for improvement, Ph.D. thesis,  
754 University of Bologna, 2017.

Collaud Coen, M., Praz, C., Haeferle, A., Ruffieux, D., Kaufmann, P., and Calpini, B.:  
756 Determination and climatology of the planetary boundary layer height above the Swiss plateau  
by in situ and remote sensing measurements as well as by the COSMO-2 model, Atmos. Chem.  
758 Phys., 14, 13205-13221, <https://doi.org/10.5194/acp-14-13205-2014>, 2014.

Dayan, U., Shenhav, R., Graber, M.: The Spatial and temporal behavior of the mixed layer in  
760 Israel, J Appl Meteorol, 27, 1382- 1394, 1988.

Dayan, U., and Koch J.: A synoptic analysis of the meteorological conditions affecting  
762 dispersion of pollutants emitted from tall stacks in the coastal plain of Israel. Atmos Environ.,  
26A, No.14, 2537-2543,1992.

764 Dayan, U., Rodnizki, J.: The temporal behavior of the atmospheric boundary layer in Israel. J  
Appl Meteorol, 38, 830-836, 1999.

766 Dayan, U., Lifshitz-Goldreich B., and Pick, K.: Spatial and structural variation of the  
atmospheric boundary layer during summer in Israel-Profiler and rawinsonde measurements.  
768 J. Appl. Meteor., 41, 447-457,2002.

- 770 [Dockery, D. W., Pope, C. A. III, Xu, X., Spengler, J. D., Ware, J. H., Fay, M. E., Benjamin G. Ferris, Jr., Speizer, F. E.: An association between air pollution and mortality in six U.S. cities. \*New England Journal of Medicine\*, 329, 1753– 1759, 1993.](#)
- 772 Doms, G., J. Förstner, E. Heise, H.-J. Herzog, D. Mironov, M. Raschendorfer, T. Reinhardt,  
774 B. Ritter, R. Schrodin, J.-P. Schulz, and G. Vogel: A description of the nonhydrostatic regional  
COSMO model. Part II: Physical parameterization. Deutscher Wetterdienst, Ofenbach, 154 pp,  
2011.
- 776 Eresmaa, N., Karppinen, A., Joffre, S. M., Räsänen, J., and Talvitie, H.: Mixing height  
determination by ceilometer, *Atmos. Chem. Phys.*, 6, 1485-1493, [https://doi.org/10.5194/acp-](https://doi.org/10.5194/acp-6-1485-2006)  
778 [6-1485-2006](https://doi.org/10.5194/acp-6-1485-2006), 2006.
- Feliks, Y.: A numerical model for estimation of the diurnal fluctuation of the inversion height  
780 due to a sea breeze, *Bound. Layer Meteor.*, 62, 151-161. 1993.
- Feliks, Y: An analytical model of the diurnal oscillation of the inversion base due to sea breeze,  
782 *J. Atmos. Sci.*, 51, 991-998,1994.
- Feliks, Y: Nonlinear dynamics and chaos in the sea and land breeze, *J. Atmos. Sci.*, 61, 2169-  
784 2187, 2004.
- 786 [Garratt, J. R.: \*The Atmospheric Boundary Layer\*, Cambridge Univ. Press, Cambridge, UK, 335 pp., 1992.](#)
- Gierens, R.T., Henriksson, S., Josipovic, M., Vakkari, V., Van Zyl, P.G., Beukes J.P., Wood,  
788 C.R., ~~Θ'Connor~~[O'Connor](#), E.J.: Observing continental boundary layer structure and evolution  
over the South African savannah using a ceilometer, *Theor. Appl. Climatol.*, 136, 333-346,  
790 <https://doi.org/10.1007/s00704-018-2484-7>, 2018.
- 792 [Goldreich Yair: \*The climate of Israel-Observations, research and applications\*, Springer US, Chap-5, 2003.](#)
- Haeffelin, M. and Angelini, F.: Evaluation of mixing height retrievals from automatic profiling  
794 lidars and ceilometers in view of future integrated networks in Europe, *Bound. Lay. Meteorol.*,  
143, 49–75, 2012.
- 796 Hanna, S. R.: The thickness of the planetary boundary layer, *Atmos. Environ.*, 3, 519–536,  
1969.

798 Hashmonay, R., Cohen, A., and Dayan, U.: Lidar observations of the atmospheric boundary  
layer in Jerusalem, *J. Appl. Meteorol.*, 30, 1228-1236, 1991.

800 [Héroux, E., Brunekreef, B., Anderson, H. R., Atkinson, R., Cohen, A., Forastiere, F.,  
Hurley F., Katsouyanni K., Krewski D., Krzyzanowski M., Ku"nzli N., Mills I., Querol X.,  
802 Ostro B., Walton, H.: Quantifying the health impacts of ambient air pollutants:  
Recommendations of a WHO/Europe project. \*International Journal of Public Health\*, 60, 619–  
804 627, 2015.](#)

Holzworth, C. G.: Estimates of mean maximum mixing depths in the contiguous United States,  
806 *Mon. Weather Rev.*, 92, 235–242, 1964.

Ketterer, C., Zieger, P., Bukowiecki, N.: *Bound. Lay. Meteo.*, 151, 317-334,  
808 <https://doi.org/10.1007/s10546-013-9897-8>, 2014.

Koehler, M., Ahlgrim, M. and Beljaars, A.: Unified treatment of dry convective and  
810 stratocumulus-topped boundary layers in the ECMWF model, *Q. J. R. Meteorol. Soc.*, 137, 43-  
57, 2011.

812 [Koch J., Dayan U.: A synoptic analysis of the meteorological conditions affecting dispersion  
of pollutants emitted from tall stacks in the coastal plain of Israel, \*Atmos Environ\*, 26A\(14\),  
814 2537-2543, 1992.](#)

Kotthaus, S. and Grimmond, C.S.B.: Atmospheric boundary-layer characteristics from  
816 ceilometer measurements. Part 1: a new method to track mixed layer height and classify clouds,  
*Q J R Meteorol. Soc.*, 144 (714), 1525–1538, <https://doi.org/10.1002/qj.3299>, 2018.

818 Levi Y., Shilo E., and Setter I.: Climatology of a summer coastal boundary layer with 1290-  
MHz wind profiler radar and a WRF simulation, *J. Appl. Meteorol. Climatol.*, 50, 1815-1826,  
820 <https://doi.org/10.1175/2011JAMC2598.1>, 2011.

Lieman, R. and Alpert, P.: Investigation of the planetary boundary layer height variations over  
822 complex terrain, *Bound. Lay. Meteorol.*, 62, 129-142, 1993.

[Ludwing F. L.: A review of coastal zone meteorological processes important to the modeling  
824 of air pollution, \*Air pollution modeling and its application IV\*, edited by C.De Wispelaere,  
NATO, Challenges of modern society, VOL 7, 1983.](#)

826 [Luo, T., Yuan R., Wang Z.: On factors controlling marine boundary layer aerosol optical depth,  
\*J. Geophys. Res. Atmos.\*, 119, 3321–3334, doi:10.1002/ 2013JD020936, 2014.](#)



828 Lyons, W.A.: Turbulent diffusion and pollutant transport in shoreline environments. Lectures  
on air pollution and environmental impact analysis, D.A. Haugen (ED.), American  
830 Meteorological Society. 136-208, 1975.

Mamouri, R.E., Ansmann, A., Nisantzi, A., Solomos, S., Kallos, G., and Hadjimitsis, D.G.:  
832 Extreme dust storm over the Eastern Mediterranean in September 2015: satellite, lidar, and  
surface observations in the Cyprus region, *Atmos. Chem. Phys.*, 16(21), 13711-13724, 2016.

834 Manninen A. J., Marke T., Tuononen M. J., O'Connor E. J.: Atmospheric boundary layer  
classification with Doppler lidar, Journal of Geophysical Research: Atmospheres, 123, 8172–  
836 8189, <https://doi.org/10.1029/2017JD028169>,2018.

Mellor M. J., and Yamada T.: Development of a turbulence closure model for geophysical fluid  
838 problems, Reviews of geophysics and space physics, 20 (4), 851-875,  
<https://doi.org/10.1029/RG020i004p00851>, 1982.

840 Neumann J.: Diurnal variations of the subsidence inversion and associated radio wave  
propagation phenomena over the coastal area of Israel. *Isr. Met. Serv*, 1952.

842 Neumann J.: On the rotation rate of the direction of sea and land breezes. *J. Atmos. Sci.*, 34,  
1913-1917, 1977.

844 Ogawa, Y., T. Ohara, S. Wakamatsu, P.G. Diosey, and I. Uno: Observations of lake breeze  
penetration and subsequent development of the thermal internal boundary layer for the  
846 Nontecore II shoreline diffusion experiment. Boundary layer meteorology, 35, 207-230,1986.

Papayannis, A., Amiridis, V., Mona, L., Tsaknakis, G., Balis, D., Bösenberg, J., Chaikovski,  
848 A., De Tomasi, F., Grigorov, I., Mattis, I. and Mitev, V.: Systematic lidar observations of  
Saharan dust over Europe in the frame of EARLINET (2000–2002). Journal of Geophysical  
850 Research: Atmospheres, 113(D10), 2008.

Saaroni, H., and Ziv B.: Summer Rainfall in a Mediterranean Climate – The Case of Israel:  
852 Climatological – Dynamical Analysis, Int. J. Climatol., 20, 191 – 209, 2000.

Scarino, A. J., Obland, M. D., Fast, J. D., Burton, S. P., Ferrare, R. A., Hostetler, C. A., Berg,  
854 L. K., Lefer, B., Haman, C., Hair, J. W., Rogers, R. R., Butler, C., Cook, A. L., and Harper, D.  
B.: Comparison of mixed layer heights from airborne high spectral resolution lidar, ground-  
856 based measurements, and the WRF-Chem model during CalNex and CARES, Atmos.  
Chem. Phys., 14, 5547–5560, [doi:10.5194/acp-14-5547-2014](https://doi.org/10.5194/acp-14-5547-2014), 2014.

858 Seidel, D. J., Ao, C. O., and Li, K.: Estimating climatological planetary boundary layer heights  
from radiosonde observations: Comparison of methods and uncertainty analysis, *J. Geophys.*  
860 *Res.*, 115, D16113, doi:10.1029/2009JD013680, 2010.

[Seidel, D., Zhang, Y., Beljaars, A., Golaz, J.-C. and Medeiros, B.: Climatology of the planetary  
862 boundary layer over continental United States and Europe, \*J. Geophys. Res.\*, 117, D17106,  
2012.](#)

864 [Sharf G., Peleg M., Livnat M, and Luria M.: Plume rise measurements from large point sources  
in Israel. \*Atmos. Environ\*, 27A, No.11, pp 1657-1663,1993.](#)

866 Steppeler J., Doms G., Schattler U., Bitzer HW, Gassmann A., Damrath U., Gregoric G.: Meso  
gamma scale forecasts by nonhydrostatic model LM. *Meteorological Atmospheric Physics*, 82,  
868 75–96, 2003.

Stull R.B.: An introduction to boundary layer meteorology, Kluwer Academic Publishers, the  
870 Netherlands, 666 p., 1988.

[Su, T., Li, Z., and Kahn, R.: Relationships between the planetary boundary layer height and  
872 1027 surface pollutants derived from lidar observations over China, \*Atmos. Chem. Phys.\*, 18,  
1028 15921-15935, 2018.](#)

874 Tiedtke, M., 1989: A Comprehensive Mass Flux Scheme for Cumulus Parameterization in  
Large-Scale Models. *Mon. Wea. Rev.*, 117, 1779–1800, <https://doi.org/10.1175/1520-0493>,  
876 1989.

Uzan, L. and Alpert, P.: The coastal boundary layer and air pollution - a high temporal  
878 resolution analysis in the East Mediterranean Coast, *The Open Atmospheric Science Journal*,  
6, 9–18, 2012.

880 -Uzan, L., Egert, S., and Alpert, P.: Ceilometer evaluation of the eastern Mediterranean summer  
boundary layer height – first study of two Israeli sites, *Atmos. Meas. Tech.*, 9, 4387–4398,  
882 <https://doi.org/10.5194/amt-9-4387-2016>, 2016.

[Von Engeln A Uzan, L., Egert, S., and Teixeira Alpert, P.: New insights into the vertical  
884 structure of the September 2015 dust storm employing eight ceilometers and auxiliary  
measurements over Israel, \*Atmos. Chem. Phys.\*, 18, 3203-3221, \[https://doi.org/10.5194/acp-  
18-3203-2018\]\(https://doi.org/10.5194/acp-<br/>886 18-3203-2018\), 2018.](#)

- 888 Van der Kamp D., McKendry I.: Diurnal and seasonal trends in convective mixed-layer heights estimated from two years of continuous ceilometer observations in Vancouver, BC. Bound Layer Meteorol, 137(3), 459–475, 2010.
- 890 Vogelezang D.H.P., and Holtslag A.A.M.: Evaluation and model impacts of alternative boundary-layer height formulations, Boundary-Layer Meteorol. 81, 245-269,1996.
- 892 Urbanski, S., Kovalev, V.A., Hao, W.M., Wold, C., Petkov, A.: Lidar and airborne investigation of smoke plume characteristics: Kootenai Creek Fire case study, Proceedings of 25th International Laser Radar Conference, St. Petersburg, Russia, Tomsk. Publishing House of IAO SB RAS. p. 1051–1054,2010.
- 894 Wang, Z., Cao, X., Zhang, L., Notholt, J. A., Zhou, B., Liu, R., and Zhang, B.: Lidar measurement of planetary boundary layer height climatology derived from ECMWF reanalysis data and comparison with microwave profiling radiometer observation, Atmos. Meas. Tech., 5, 1965–1972, <https://doi.org/10.5194/amt-5-1965-2012>, 2012.
- 900 Wetzel P.J. Climate., 126, 6575–6590, <https://doi.org/10.1175/JCLI-D-12-00385>, 2013.: Toward parametrization of the stable boundary layer, J. Appl. Meteorol. 21, 7-13, 1982.
- 902 Wiegner M., Madonna F., Biniotoglou I., Forkel R., Gasteiger J., Geiß A., Pappalardo G., Schäfer K., and Thomas W.: What is the benefit of ceilometers for aerosol remote sensing? An answer from EARLINET, Atmos. Meas. Tech., 7, 1979–1997, <https://doi.org/10.5194/amt-7-1979-2014>, 2014.
- 904
- 906 Wiegner, M. and Gasteiger, J.: Correction of water vapor absorption for aerosol remote sensing with ceilometers, Atmos. Meas. Tech., 8, 3971–3984, [https://doi.org/10.5194/amt-8-3971-](https://doi.org/10.5194/amt-8-3971-2015)
- 908 2015, 2015.
- 910 Yuval, Dayan, U., Levy, I., & Broday, D. M: On the association between characteristics of the atmospheric boundary layer and air pollution concentrations, Atmospheric Research, [doi.org/10.1016/j.atmosers.2019.104675](https://doi.org/10.1016/j.atmosers.2019.104675), 2019.
- 912 Zhang, Y., Gao, Z., Li, D., Li, Y., Zhang, N., Zhao, X., and Chen, J.: On the computation of planetary boundary-layer height using the bulk Richardson number method, Geosci. Model Dev., 7, 2599-2611, <https://doi.org/10.5194/gmd-7-2599-2014>, 2014.
- 914
- 916 Ziv B., Saaroni H., and Alpert P.: The factors governing the summer regime of the eastern Mediterranean, Intern. J. of Climatol., 24, 1859-1871, 2004.

918 Table 1. Location of measurements sites and ceilometer types and type of ceilometers

| Location                                                                                              | Site                  | Long/Terrain      | Lat/Lon | Distance from  | Height                                  |
|-------------------------------------------------------------------------------------------------------|-----------------------|-------------------|---------|----------------|-----------------------------------------|
| Ceilometer type                                                                                       |                       |                   |         |                |                                         |
| <u>MD<sub>c</sub> shoreline (km) (m a.s.l) (resolution, height limit, max range<sub>a</sub>) (km)</u> |                       |                   |         |                |                                         |
| Ramat David (RD)                                                                                      | <u>NorthPlain</u>     | 32.7 °/35.2 °     | 24      | <u>50</u>      | <u>CL31 (10 m, 16 s, up to 7.7 km)</u>  |
| Hadera (HD)                                                                                           | <u>ShorelineCoast</u> | 32.5 °/34.9 °     | 3.5     | <u>10</u>      | <u>CL31 (10 m, 16 s, up to 7.7 km)</u>  |
| Tel Aviv (TLV)                                                                                        | <u>ShorelineCoast</u> | 32.1 °/34.8 °     | 0.05    | <u>5</u>       | <u>CL31 (10 m, 16 s, up to 7.7 km)</u>  |
| <u>BeitBet</u> Dagan (BD) <sub>b</sub>                                                                | <u>InlandPlain</u>    | 32.0 °/34.8 °     | 7.5     | 33             | <u>CL31 (10 m, 15 s, up to 7.7 km)</u>  |
| Weizmann (WZ)                                                                                         | <u>InlandPlain</u>    | 31.9 °/34.8 °     | 11.5    | <u>60</u>      | <u>CL51 (10 m, 16 s, up to 15.4 km)</u> |
| Jerusalem ( <u>JRM</u> )                                                                              | <u>MountainMoun</u>   | 31.8 °/35.2 °     | 53      | <u>830</u>     | <u>CL31 (10 m, 16 s, up to 7.7 km)</u>  |
| <u>Nevatim</u> ( <u>NVHazerim</u> (HZ))                                                               | <u>SouthAr</u>        | 31.2 °/34.96 °    | 44      | <u>400 200</u> | <u>CL31 (10 m, 16 s, up to 7.7 km)</u>  |
| <u>Hazerim</u> ( <u>HZNevatim</u> (NV))                                                               | <u>SouthAr</u>        | 31.2 °/34.735.0 ° | 70      | <u>200 400</u> | <u>CL31 (10 m, 16 s, up to 7.7 km)</u>  |

<sup>a</sup>The maximum height limit depends on sky conditions and decreases as the atmospheric optical density (AOD) increases. Data acquisition was limited

<sup>b</sup>Adjacent to 4.5 km by the ceilometers' software (BLview), except in Beit Dagan.

<sup>b</sup>The location of ceilometer Beit Dagan and the radiosonde launch site.

<sup>c</sup>Mediterranean

924

926

928

930

932 Table 2. ParametersDescription of the NWP models

| <u>Model</u>                                |               |                         |                         | <u>IFS</u>                                         | <u>COSMO</u>                                                                                      |
|---------------------------------------------|---------------|-------------------------|-------------------------|----------------------------------------------------|---------------------------------------------------------------------------------------------------|
| <u>Convection parametrization</u>           | <u>Type</u>   | <u>Resolution (deg)</u> | <u>Operation center</u> | <u>ECMWF</u>                                       | <u>IMS</u>                                                                                        |
| <u>Mass flux Tiedtke shallow convection</u> |               |                         |                         | <u>Global</u>                                      | Regional, boundary conditions from IFS                                                            |
| <u>Global/regional</u>                      |               |                         |                         |                                                    | 0.025°                                                                                            |
| <u>Mass flux Tiedtke-Bechtold</u>           | <u>Global</u> |                         |                         | 0.125° in 2015 (~13km)                             | <u>IFS</u>                                                                                        |
| <u>Horizontal grid resolution</u>           |               |                         |                         | 0.125° in 2016 (~9 km)                             |                                                                                                   |
| <u>Vertical grid resolution</u>             |               |                         |                         | 137 layers up to ~79 km                            | 60 layers up to 23.5 km                                                                           |
|                                             |               |                         |                         | 23 lie within the first 3 km                       | 20 lie within the first 3 km                                                                      |
| <u>Temporal resolution of the output</u>    |               |                         |                         | <u>Hourly profiles</u>                             | <u>15 min profiles</u>                                                                            |
| <u>Convection parametrization</u>           |               |                         |                         | <u>Mass flux Tiedtke-Bechtold (Bechtold, 2008)</u> | <u>Deep convection resolved. Parametrization of mass flux shallow convection. (Tiedtke, 1989)</u> |

934

936

938

940

942

944 ~~Table 3. Statistical analysis of the Beit Dagan PBL heights on 33 summer days (13 days on~~  
 946 ~~August 2015 and 20 days on August 2016) from IFS and COSMO models by the bulk~~  
 948 ~~Richardson method (IFS<sub>R</sub>, COSMO<sub>R</sub>), the parcel method (IFS<sub>P</sub>, COSMO<sub>P</sub>) and the WCT~~  
~~method for the adjacent ceilometer. The PBL heights were compared to those derived from~~  
~~Beit Dagan radiosonde by either the parcel or bulk Richardson methods (same results, see Fig~~  
~~2).~~

Table 3. Statistical analysis of Bet Dagan PBL heights (N=91, Fig. 2a)

| PBL<br>detectio<br>n     | <u>IFS<sub>R</sub>IFS</u><br><u>-pm</u> | <u>IFS<sub>P</sub>COSMO</u><br><u>-pm</u> | <u>COSMO<sub>R</sub>IFS</u><br><u>-ri</u> | <u>COSMO<sub>P</sub>COSMO</u><br><u>-ri</u> | Ceilomete<br>r | <u>RS</u>             |
|--------------------------|-----------------------------------------|-------------------------------------------|-------------------------------------------|---------------------------------------------|----------------|-----------------------|
| Mean                     |                                         | <u>27152</u>                              | <u>-3366</u>                              | <u>-10657</u>                               | <u>-124</u>    | <u>-</u>              |
| Error<br>(m)             | <u>274346</u>                           |                                           |                                           |                                             |                |                       |
| RMSE<br>(m)              | <u>432494</u>                           | <u>411146</u>                             | <u>152579</u>                             | <u>-176193</u>                              | <u>-97143</u>  | <u>-</u>              |
| R                        | <u>0.4814</u>                           | <u>0.2184</u>                             | <u>-0.8313</u>                            | <u>0.837</u>                                | <u>0.9383</u>  | <u>-</u>              |
| Mean<br>PBL-(m<br>a.s.l) | <u>-1250</u><br><u>1236</u>             | <u>1247838</u>                            | <u>-9731255</u>                           | <u>869947</u>                               | <u>989894</u>  | <u>89</u><br><u>0</u> |
| Std<br>PBLST<br>D (m)    |                                         | <u>-245237</u>                            | <u>-273346</u>                            | <u>-222232</u>                              | <u>259239</u>  | <u>24</u><br><u>5</u> |

950

952

954

956

958

960 Table 4. Root mean square errors of PBL heights from five sites on 13 summer days (Fig. 4),  
 962 derived by IFS and COSMO models by the bulk Richardson method ( $IFS_R$ ,  $COSMO_R$ ) and the  
 parcel method ( $IFS_P$ ,  $COSMO_P$ ). The PBL heights were compared to the heights measured by  
 the Beit Dagan ceilometer.

964 Table 4. Statistical analysis of Tel Aviv PBL heights (N=122, Fig. 3a)

| Site        | PBL detection                          | $IFS_P$      | $COSMO_P$ | $COSMO_R$ | $COSMO_P$ | Ceilomet |
|-------------|----------------------------------------|--------------|-----------|-----------|-----------|----------|
|             |                                        | $IF$         | $-pm$     | $FS-ri$   | $O-ri$    | $er$     |
|             |                                        | $S-pm$       |           |           |           |          |
| Ramat David | 173<br>m<br>Mea<br>n<br>Error<br>(m)   | 180<br>m14   | 247 m17   | 232 m436  | 18        | -        |
| Tel Aviv    | 276<br>RMSE<br>(m)                     | 498<br>m256  | 203 m183  | 182 m616  | 180       | -        |
| Beit Dagan  | R                                      | 405<br>m0.47 | 569 m0.74 | 235 m0.03 | 171 m0.73 | -        |
| Weizman     | n<br>214<br>m<br>Mea<br>n (m<br>a.s.l) | 339<br>m702  | 175 m706  | 209 m1124 | 707       | 674      |
| Jerusalem   | m<br>351<br>STD<br>(m)                 | 285<br>m224  | 251 m238  | 179 m337  | 211       | 258      |

966

968

970

972

974

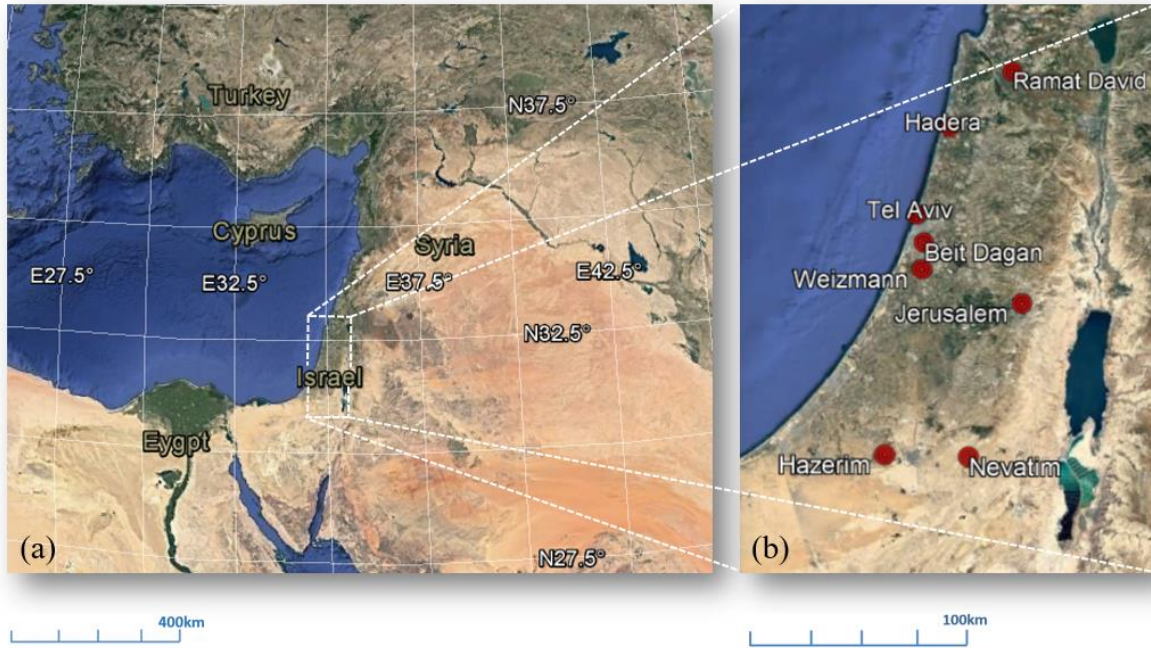
Table 5. Same as in Table 3 but for mean errors. Statistical analysis of Ramat David PBL heights (N=123, Fig. 4a)

| <u>Site</u>      | <u>PBL</u>            | <u>IFS<sub>R</sub></u> | <u>IFS<sub>P</sub></u> | <u>COSM<sub>R</sub></u> | <u>COSM<sub>P</sub></u> | <u>Ceilom</u> |
|------------------|-----------------------|------------------------|------------------------|-------------------------|-------------------------|---------------|
| <u>detection</u> | <u>pm</u>             | <u>O-pm</u>            | <u>IFS-ri</u>          | <u>O-ri</u>             | <u>eter</u>             |               |
| Ramat David      | 34<br>Mean Error (m)  | -0.4                   | -26.4                  | -12.4                   | 123                     | -             |
| Tel Aviv         | 234<br>RMS E (m)      | 422.3                  | 19.2                   | -35.7                   | 313                     | -             |
| Beit Dagan       | R                     | 49.1<br>332.7<br>m0.1  | -0.55<br>m             | -0.08                   | 0.39                    | -             |
| Weizman          | 114<br>Mean (m a.s.l) | 280.9                  | 16.1                   | -42.1                   | 1114                    | 991           |
| Jerusalem        | 298<br>STD (m)        | 243.2                  | -6.2                   | -1.5                    | 268                     | 253           |

976

978





980 Table 6. Statistical analysis of Weizmann PBL heights (N=55, Fig. 5a)

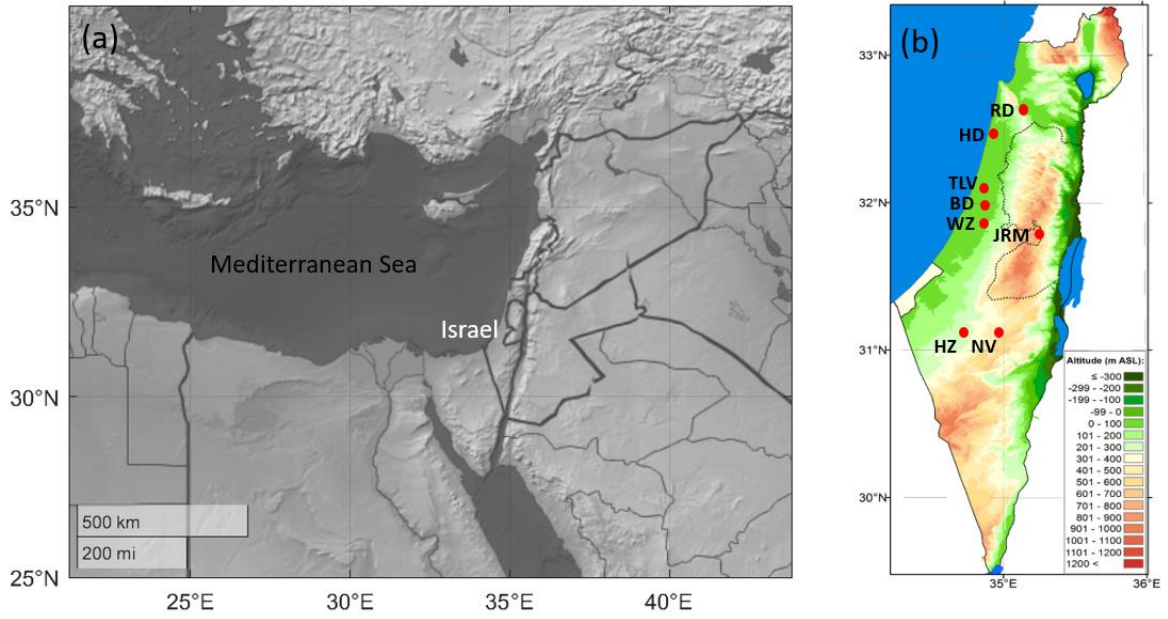
| <u>PBL detection</u>  | <u>IFS-pm</u> | <u>COSMO-pm</u> | <u>IFS-ri</u> | <u>COSMO-ri</u> | <u>Ceilometer</u> |
|-----------------------|---------------|-----------------|---------------|-----------------|-------------------|
| <u>Mean Error (m)</u> | <u>67</u>     | <u>-106</u>     | <u>430</u>    | <u>21</u>       | <u>-</u>          |
| <u>RMSE (m)</u>       | <u>162</u>    | <u>207</u>      | <u>604</u>    | <u>192</u>      | <u>-</u>          |
| <u>R</u>              | <u>0.85</u>   | <u>0.76</u>     | <u>-0.01</u>  | <u>0.72</u>     | <u>-</u>          |
| <u>Mean (m a.s.l)</u> | <u>892</u>    | <u>719</u>      | <u>1256</u>   | <u>846</u>      | <u>825</u>        |
| <u>STD (m)</u>        | <u>186</u>    | <u>193</u>      | <u>322</u>    | <u>219</u>      | <u>271</u>        |

982 Table 7. Statistical analysis of Jerusalem PBL heights (N=53, Fig. 6a)

| <u>PBL detection</u>  | <u>IFS-pm</u> | <u>COSMO-pm</u> | <u>IFS-ri</u> | <u>COSMO-ri</u> | <u>Ceilometer</u> |
|-----------------------|---------------|-----------------|---------------|-----------------|-------------------|
| <u>Mean Error (m)</u> | <u>366</u>    | <u>-129</u>     | <u>117</u>    | <u>-44</u>      | <u>-</u>          |
| <u>RMSE (m)</u>       | <u>498</u>    | <u>252</u>      | <u>257</u>    | <u>239</u>      | <u>-</u>          |
| <u>R</u>              | <u>0.18</u>   | <u>0.63</u>     | <u>0.59</u>   | <u>0.70</u>     | <u>-</u>          |
| <u>Mean (m a.s.l)</u> | <u>2239</u>   | <u>1744</u>     | <u>1991</u>   | <u>1830</u>     | <u>1874</u>       |
| <u>STD (m)</u>        | <u>276</u>    | <u>253</u>      | <u>258</u>    | <u>328</u>      | <u>250</u>        |

984 Table 8. Statistical analysis of Nevatim PBL heights (N=72, Fig. 7a)

| <u>PBL detection</u>      | <u>IFS-pm</u> | <u>COSMO-pm</u> | <u>IFS-ri</u> | <u>COSMO-ri</u> | <u>Ceilometer</u> |
|---------------------------|---------------|-----------------|---------------|-----------------|-------------------|
| <u>Mean Error (m)</u>     | <u>149</u>    | <u>186</u>      | <u>214</u>    | <u>264</u>      | <u>-</u>          |
| <u>RMSE (m)</u>           | <u>423</u>    | <u>436</u>      | <u>369</u>    | <u>488</u>      | <u>-</u>          |
| <u>R</u>                  | <u>0.1</u>    | <u>0.15</u>     | <u>0.30</u>   | <u>0.23</u>     | <u>-</u>          |
| <u>Mean PBL (m a.s.l)</u> | <u>1728</u>   | <u>1756</u>     | <u>1792</u>   | <u>1843</u>     | <u>1579</u>       |
| <u>STD PBL (m)</u>        | <u>341</u>    | <u>352</u>      | <u>268</u>    | <u>394</u>      | <u>237</u>        |



986 Fig. 1 Maps of (a) the East Mediterranean (a), and (b) the research area including study region  
 988 in Israel (b), with indications of the ceilmeters-ceilmeters' measurement sites (red circles).  
 989 The Radiosonde launch site is situated in Beit, details given in Table 1) on a topography map  
 990 adapted from © Israeli meteorological service.

990 .

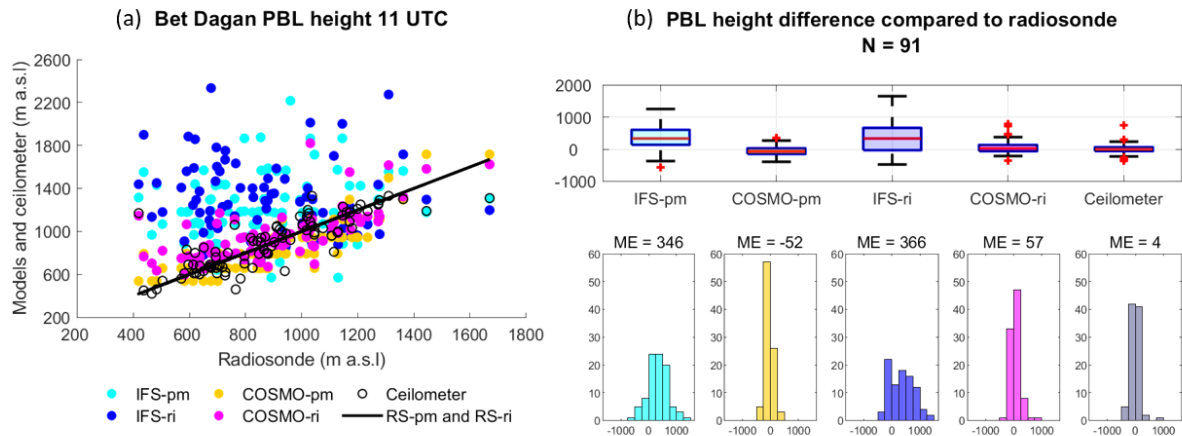
992

994

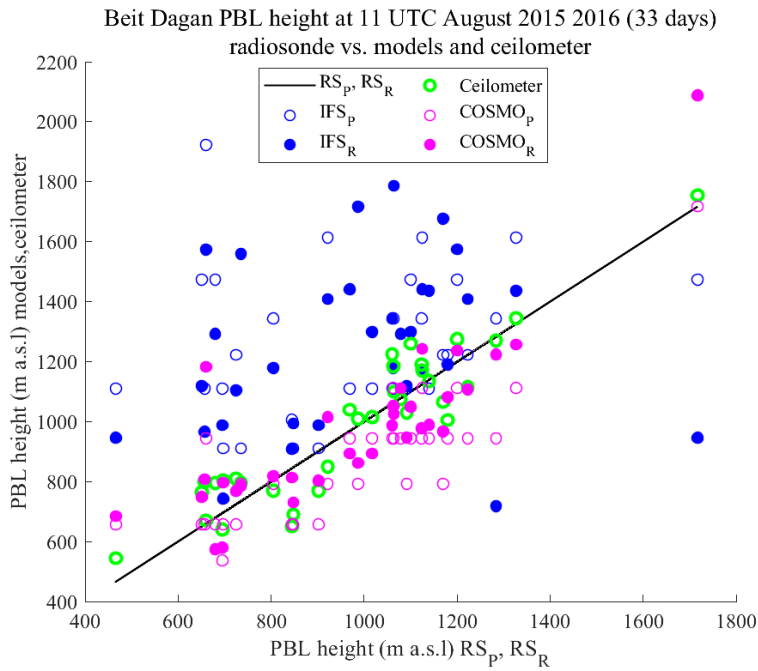
996

998

1000

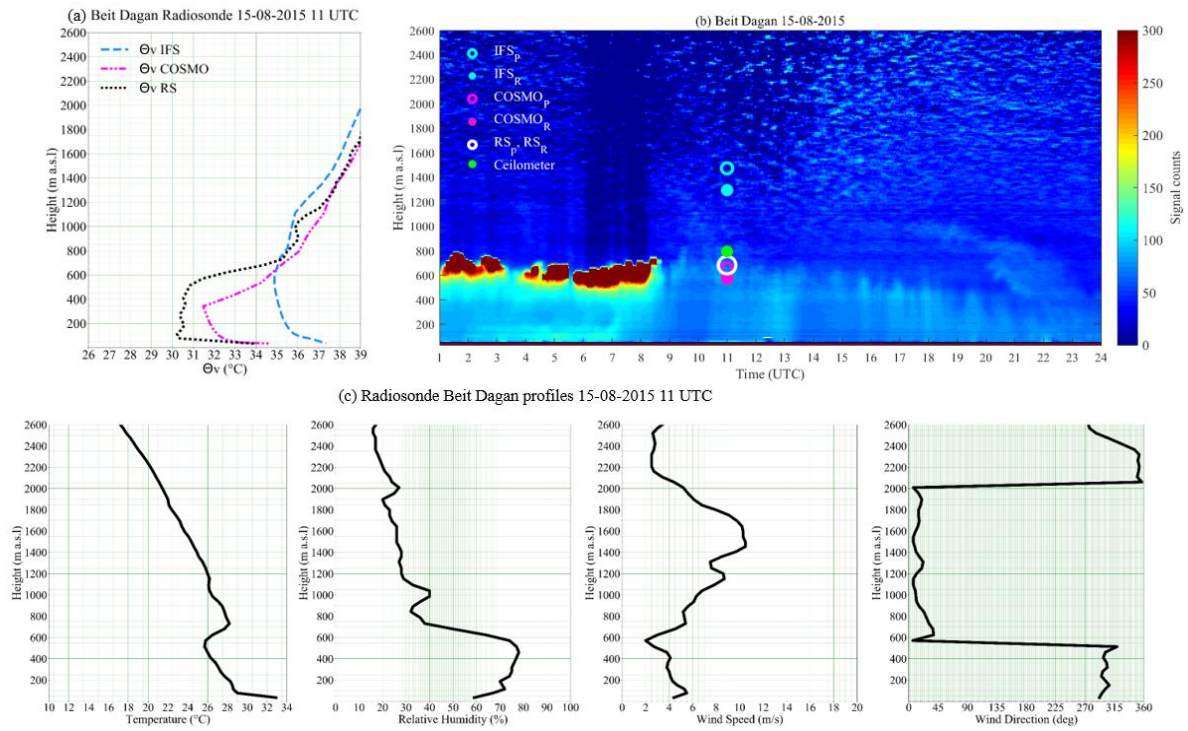


1002 Fig. 2 PBL height from Bet Dagan, adjacent to the ceilometer. Adapted from © Google Maps  
 1004 2019, site at 11 UTC on 91 days for periods of July-September 2015 and June-September 2016.  
 1006 Ceilometer profiles analyzed by the WCT method. The IFS, COSMO, and radiosonde profiles  
 1008 analyzed by the bulk Richardson method (RS-ri, IFS-ri, COSMO-ri) and the parcel method  
 1010 (RS-pm, IFS-pm, COSMO-pm). The results compared to the radiosonde (RS-ri and RS-pm  
 1012 produced the same heights). Statistical analysis of the scatter plot (a) is given in Table 3. PBL  
 1014 height difference presented by boxplots and histograms (b). The edges of the boxplot are the  
 1016 25th and 75th percentiles (q1 and q3), the whiskers enclose all data points not considered  
 1018 outliers (red crosses). A central red line indicates the median. Each boxplot is described by a  
 1020 histogram beneath.



1022

1024 Fig. 2. PBL heights over Beit Dagan site on 33 summer days (13 days on August 2015 and 20  
 1026 days on August 2016), generated by the bulk Richardson method for IFS model (IFS<sub>R</sub>, blue  
 1028 solid circles), COSMO model (COSMO<sub>R</sub>, pink solid circles), and Beit Dagan radiosonde  
 1030 profiles (RS<sub>R</sub>, black line). PBL heights generated by the parcel method for the IFS model (IFS<sub>P</sub>,  
 open blue circles), COSMO model (COSMO<sub>P</sub>, open pink circles), and Beit Dagan radiosonde  
 profiles (RS<sub>P</sub>, same black line as RS<sub>R</sub>, the results are identical). PBL heights derived from the  
 Beit Dagan ceilometer were produced by the WCT method (green circles). Extreme Results  
 (up to ~2,00 m a.s.l) for August 17, 2016, are shown on the right hand side.



1032

Fig.3 Meteorological measurements from Beit Dagan site on August 15, 2015: Virtual potential temperature profiles at 11 UTC generated from radiosonde measurements, IFS and COSMO models (a), ceilometer signal counts plot including indications of the PBL heights at 11 UTC from the models (IFS<sub>R</sub>, IFS<sub>P</sub>, COSMO<sub>R</sub>, COSMO<sub>P</sub>), radiosonde (RS<sub>R</sub>, RS<sub>P</sub>) and ceilometer (b). The bottom panel presents radiosonde profiles of temperature, RH, wind speed and wind direction at 11 UTC (c).

1034

1036

1038

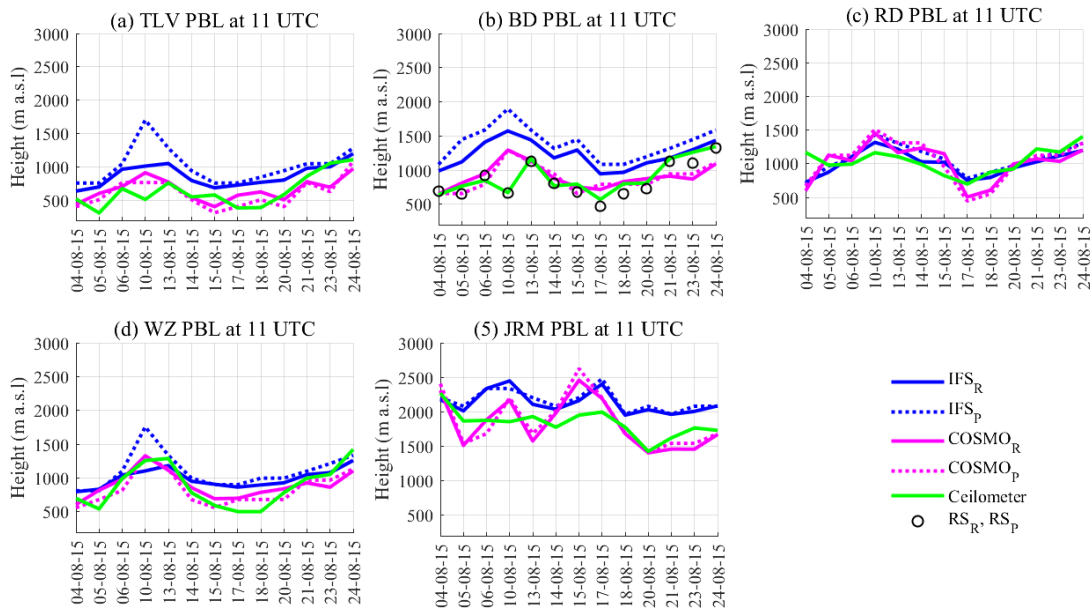
1040

1042

1044

1046

1048



1050

1052 **Fig. 4** PBL heights on 13 August days in 2015 from five ceilometer sites: (a) Tel Aviv (TLV),  
 1054 (b) Beit Dagan (BD), (c) Ramat David (RD), (d) Weizmann (WZ), and (e) Jerusalem (JRM).  
 1056 PBL heights were generated by the bulk Richardson method for the IFS model ( $IFS_R$ , blue solid  
 1058 line) and the COSMO model ( $COSMO_R$ , pink solid line). PBL heights generated by the parcel  
 1060 method for the IFS model ( $IFS_P$ , blue dashed line) and the COSMO model ( $COSMO_P$ , pink  
 1062 dashed line). Beit Dagan radiosonde profiles ( $RS_R$ ,  $RS_P$ , black circles). PBL heights derived  
 1064 from the ceilometers (green line) were produced by the WCT method.

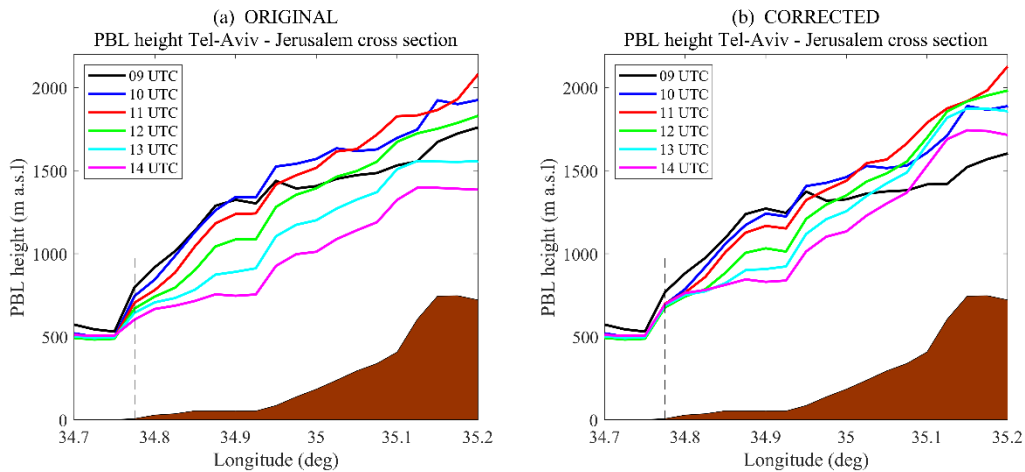
1058

1060

1062

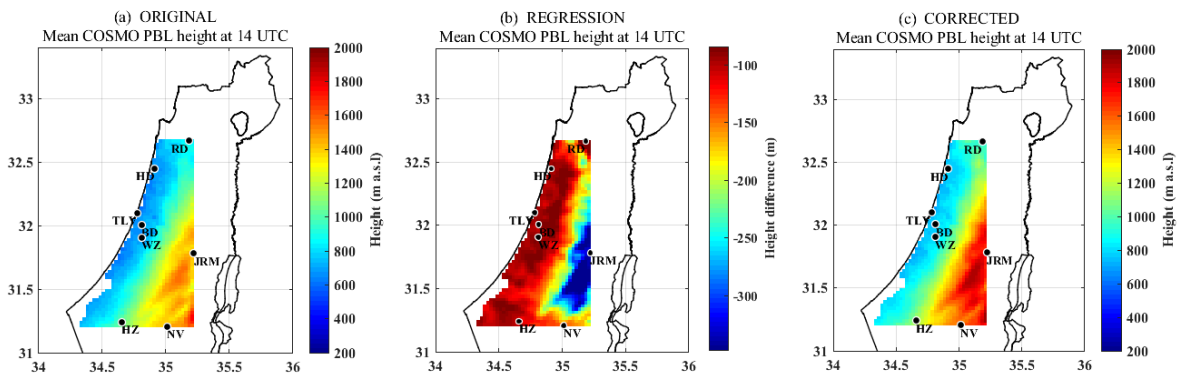
1064

1066



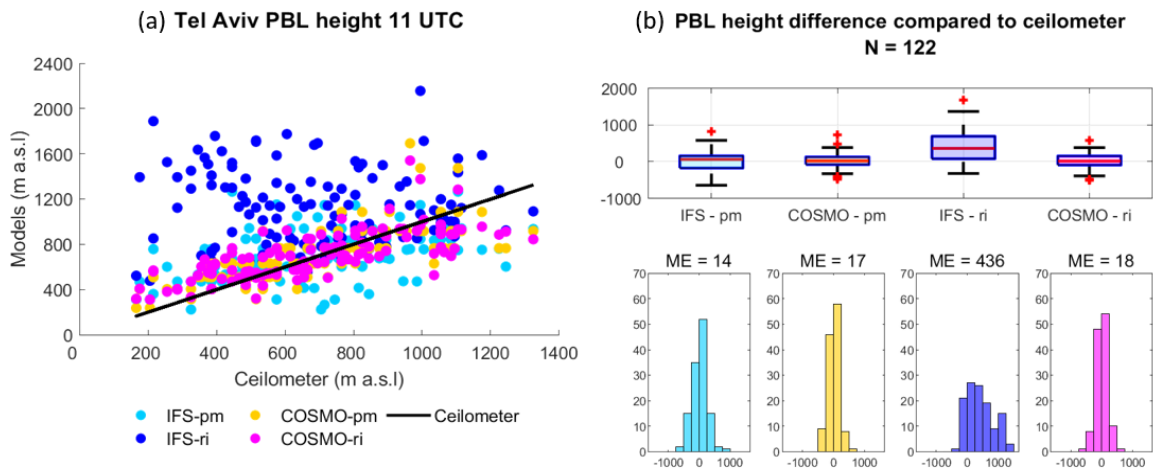
1068

1070 **Fig. 5** COSMO<sub>R</sub> mean PBL height cross-section from Tel Aviv to Jerusalem before (a) and  
 1072 after (b) correction between 9–14 UTC. The analysis was performed on the number of available  
 1074 days for each site on August 2015 as follows: Jerusalem—21 days, Nevatim—13 days, Hazerim  
 —20 days, Ramat David—26 days, Weizmann—25 days, Beit Dagan—13 days, Hadera—16  
 days, Tel Aviv—25 days. Indications of the seashore (dashed line) and the topography (brown  
 area) are given.



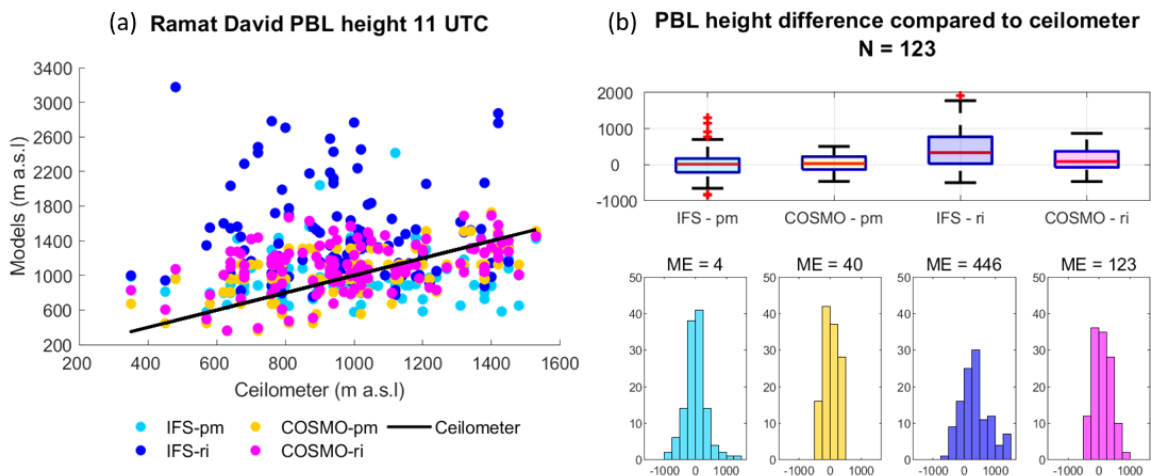
1076

1078 **Fig. 6** 3D maps of COSMO<sub>R</sub> mean PBL heights over Israel at 14 UTC before (a), and after (c)  
 1080 correction. The regression (b) based on Eq. (6), depicts the height difference between the results  
 from COSMO<sub>R</sub> and the ceilometers. The analysis was performed on the number of available  
 days for each site on August 2015 as follows: Jerusalem—21 days, Nevatim—13 days, Hazerim  
 —20 days, Ramat David—26 days, Weizmann—25 days, Beit Dagan—13 days, Hadera—16



1084 Fig. 3 Same as Fig. 2 but for Tel Aviv on 122 days. The models were compared to the ceilometer.

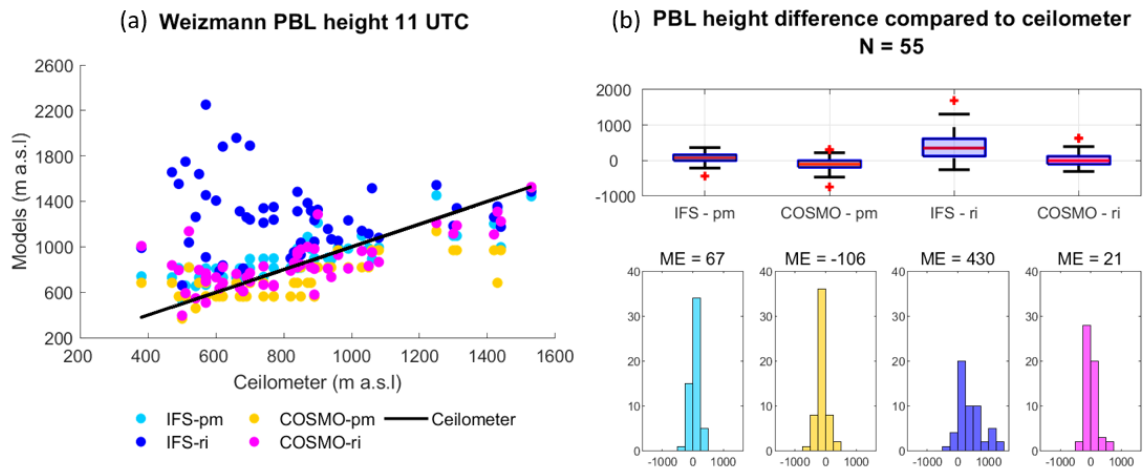
1086



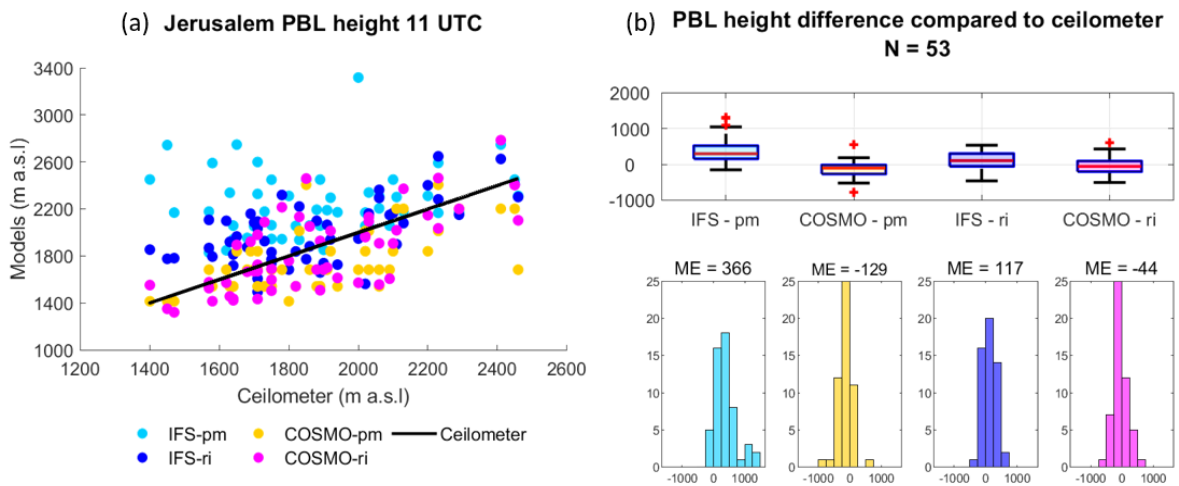
1088 Fig. 4 Same as Fig. 2 but for Ramat David on 123 days. The models were compared to the ceilometer.

1090

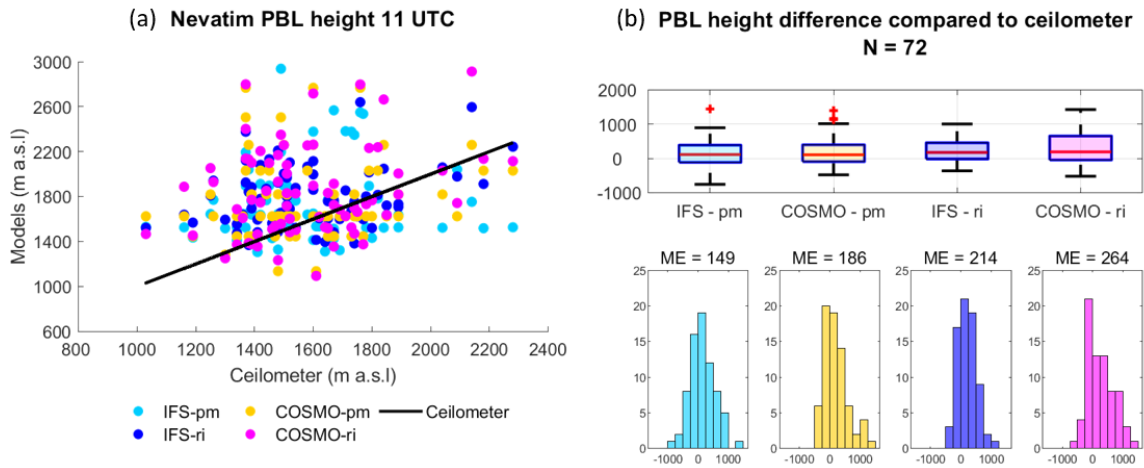




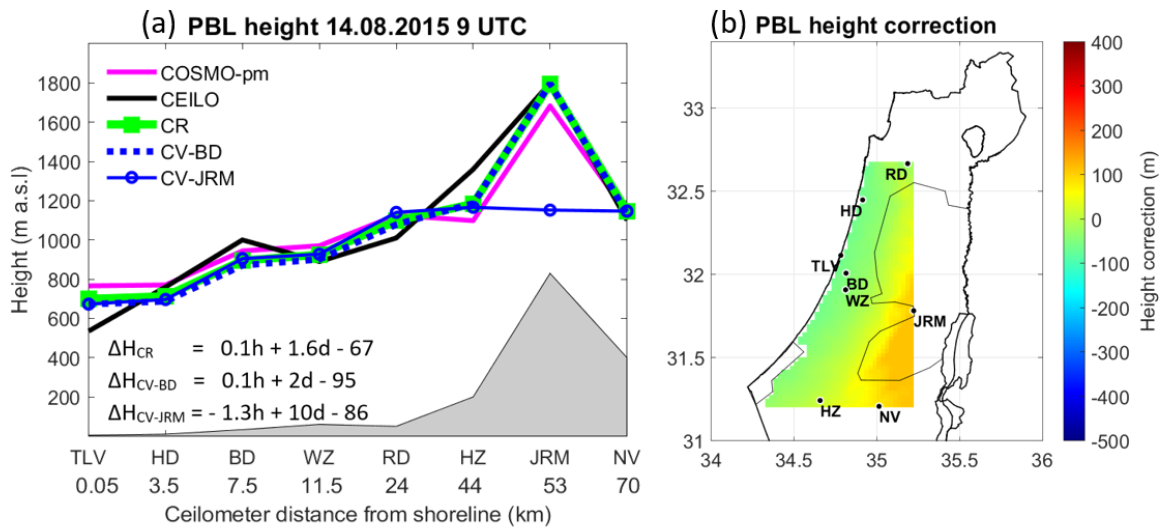
1092 Fig. 5 Same as Fig. 2 but for Weizmann on 55 days. The models were compared to the  
 1094 ceilometer.



1096 Fig. 6 Same as Fig. 2 but for Jerusalem on 53 days. The models were compared to the  
 1098 ceilometer.

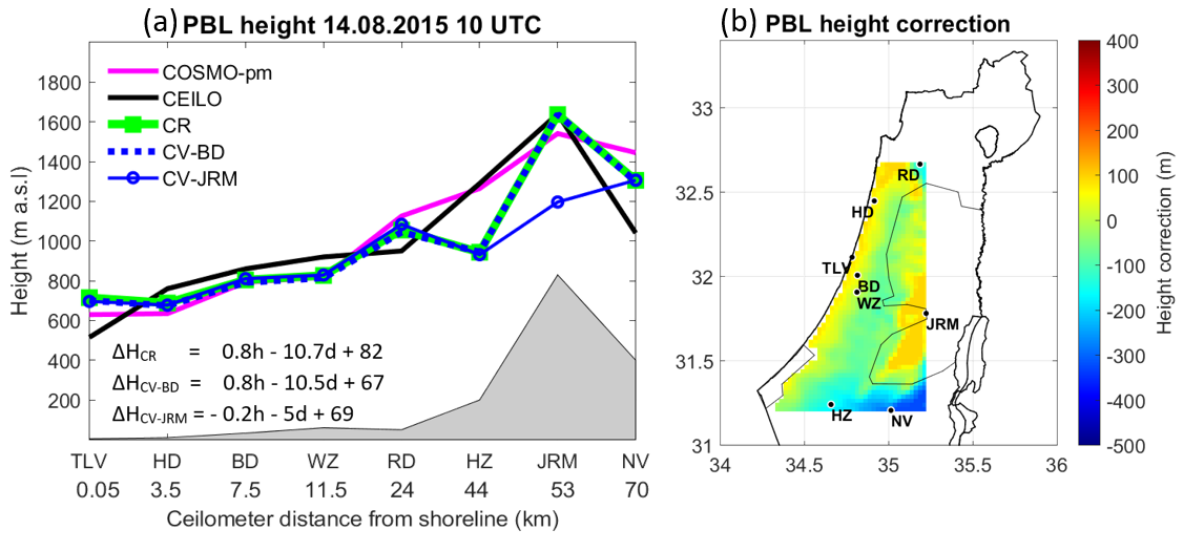


1100 Fig. 7 Same as Fig. 2 but for Nevatim on 72 days. The models were compared to the ceilometer.



1102

1104 Fig. 8 PBL heights on August 14, 2015, at 9 UTC. The left panel (a) presents an east-west  
 1106 cross-section map, according to the ceilometers' distance from the Mediterranean shoreline.  
 1108 The PBL heights were derived from COSMO-pm (pink line), the ceilometers (black line), the  
correction tool for COSMO-pm (CR, green line), cross-validation for Bet Dagan (CV-BD,  
dashed blue line), and cross-validation for Jerusalem (CV-JRM, blue circles). The right panel  
(b) shows a 2-D map (b) of the height correction range, corresponding to figure (a).



1110

Fig. 9 Same as Fig. 8 but for 10 UTC.

1112

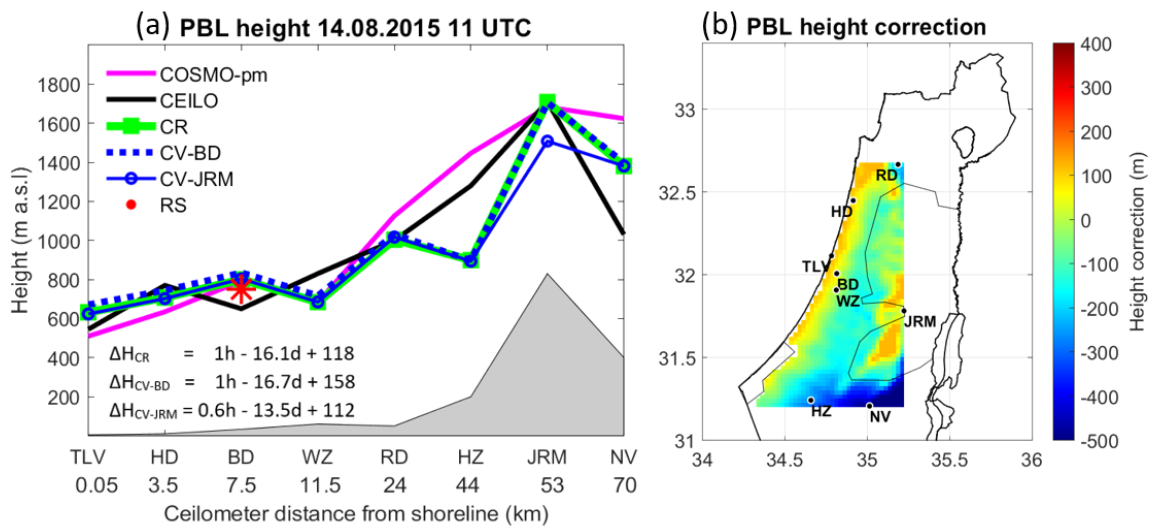
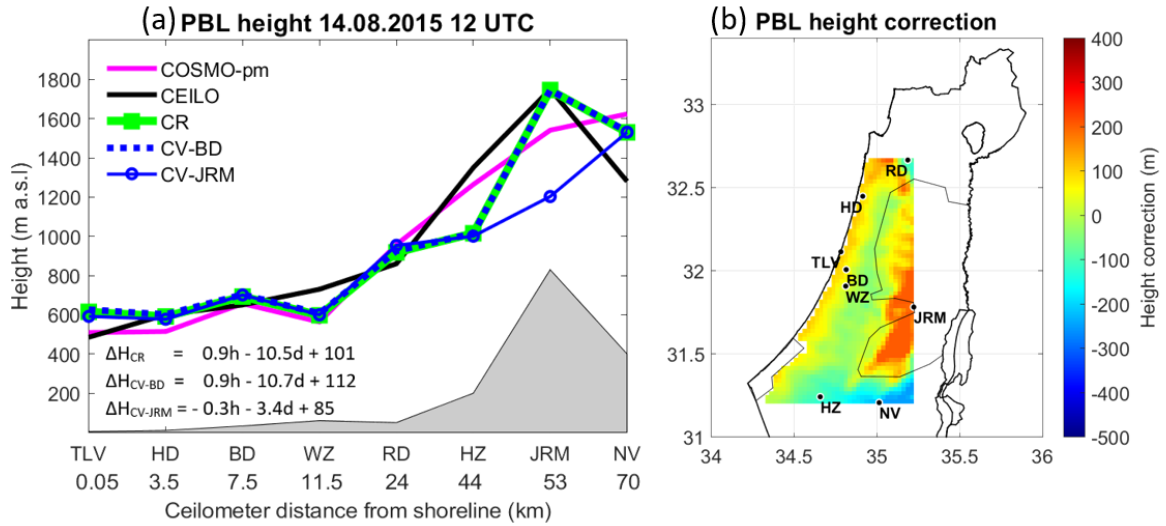
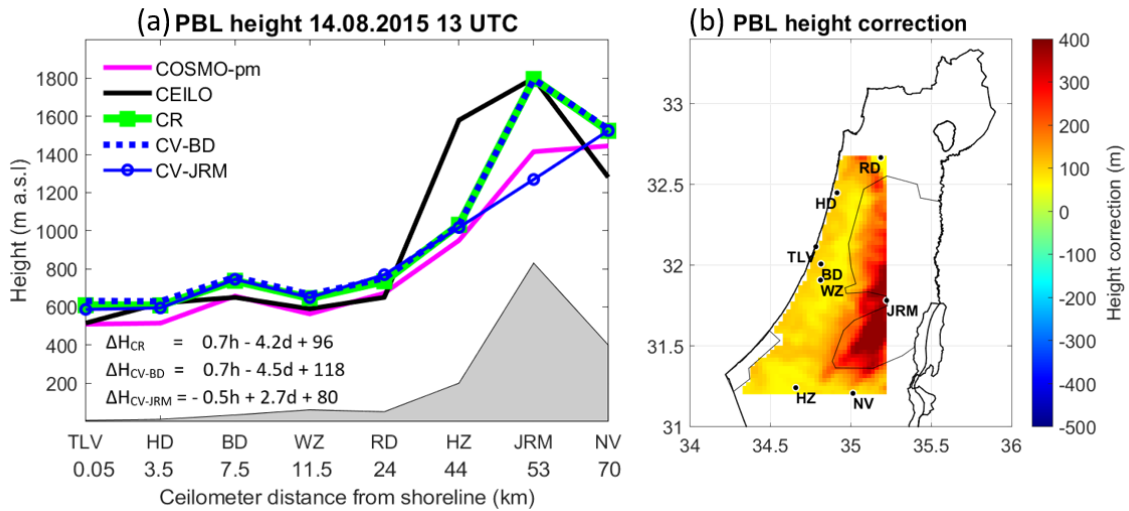


Fig. 10 Same as Fig. 8 but for 11 UTC and including the PBL height estimation from the radiosonde (red star).

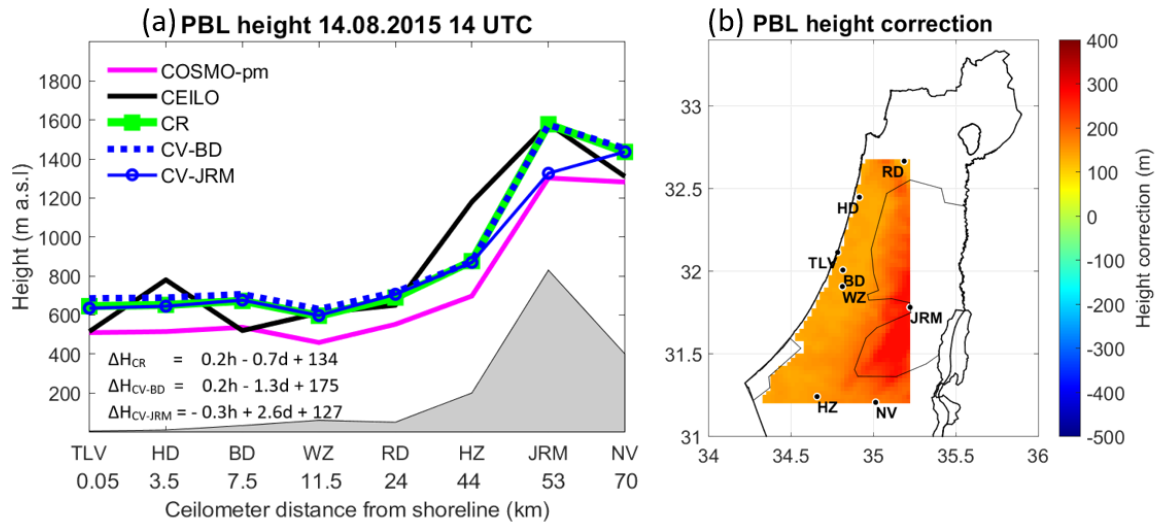
1116



1118 Fig. 11 Same as Fig. 8 but for 12 UTC.



1120 Fig. 12 Same as Fig. 8 but for 13 UTC.



1122

Fig. 13 Same as Fig. 8 but for 14 UTC.

1124

1126